CLIMATIC SENSITIVITIES DERIVED FROM TREE RINGS IMPROVE PREDICTIONS OF THE FOREST VEGETATION SIMULATOR GROWTH AND YIELD MODEL

by

Courtney Lyn Giebink

A Thesis Submitted to the Faculty of the

DEPARTMENT OF ECOLOGY AND EVOLUTIONARY BIOLOGY

In Partial Fulfillment of the Requirements
For the Degree of

MASTER OF SCIENCE

In the Graduate College

THE UNIVERSITY OF ARIZONA

2021

THE UNIVERSITY OF ARIZONA
GRADUATE COLLEGE

As members of the Master's Committee, we certify that we have read the thesis prepared by: Courtney Lyn Giebink, titled: Climatic sensitivities derived from tree rings improve predictions of the Forest Vegetation Simulator growth and yield model and recommend that it be accepted as fulfilling the thesis requirement for the Master's Degree.

Margaret Evans
Margaret E. K. Evans — Date: May 7, 2021

Judith Bronstein — Date: May 7, 2021

Scott R. Saleska — Date: May 7, 2021

R. Justin DeRose — Date: May 7, 2021

Final approval and acceptance of this thesis is contingent upon the candidate's submission of the final copies of the thesis to the Graduate College.

I hereby certify that I have read this thesis prepared under my direction and recommend that it be accepted as fulfilling the Master's requirement.

Margaret Evans
Margaret E. K. Evans — Date: May 26, 2021
Master's Thesis Committee Chair
Laboratory of Tree Ring Research

ACKNOWLEDGEMENTS

I thank John D. Shaw, R. Justin DeRose and the Utah State University lab for contributing processed tree-ring data as well as the USDA Forest Service for inventory data. Further, I thank John D. Shaw and R. Justin DeRose as well as Mark Castle for contributing expertise and advice in forest modeling. I acknowledge the World Climate Research Programme's Working Group on Coupled Modelling, which is responsible for CMIP, and I thank the climate modeling groups (listed in Table A1) for producing and making available their model output. For CMIP the U.S. Department of Energy's Program for Climate Model Diagnosis and Intercomparison provides coordinating support and led development of software infrastructure in partnership with the Global Organization for Earth System Science Portals. Finally, I thank code contributions from Jeff Oliver, Kelly Heilman, Margaret E.K. Evans, Mark Castle, and Michiel Pillet.

A special thanks to my adviser, Margaret E.K. Evans, for her mentorship. I am appreciative of the support that she provided, giving me the motivation to push through several challenges, and I am grateful for the many professional opportunities she provided me, allowing me to connect with both scientists and practitioners. I also thank my committee, Judith Bronstein, Scott Saleska, and R. Justin DeRose, for their feedback and advice. Finally, I thank the M.E.K. Evans lab for their guidance and feedback on many projects from my personal website to my thesis.

I also thank the support from my family. I thank my parents for their emotional support through the ups and downs of the past several years. Last but surely not least, I thank my husband and partner, Noah, for asking clarifying questions, diving deep with me into my work and also pulling me far away from my work, whether it was accompanying me on an ice cream run or a camping trip.

TABLE OF CONTENTS

TABLE OF CONTENTS – *Continued*

LIST OF FIGURES

LIST OF FIGURES – *Continued*

LIST OF FIGURES – *Continued*

LIST OF FIGURES – *Continued*

LIST OF TABLES

ABSTRACT

Forests have the potential, in particular through targeted management, to contribute to the stabilization and drawdown of greenhouse gases via carbon sequestration and storage. To identify management actions that will maximize carbon drawdown over the long term, foresters need models that accurately and precisely represent forest responses to changing climate. The most widely used growth and yield model in the US, the Forest Vegetation Simulator (FVS), does not include the direct effect of climate variation on tree growth. We incorporated the effects of climate on tree diameter growth by combining tree-ring data with forest inventory data to parameterize a suite of alternative models of the growth of three dominant tree species in the arid and generally climate-limited U.S. state of Utah. These species, *Pinus ponderosa*, *Pseudotsuga menziesii* var. *glauca*, and *Picea engelmannii*, encompass the full elevational range of montane forest types. The alternative models differ progressively from the current decadal time-step FVS large-tree diameter growth model, first through changing to an annual time step, then by adding interannual climate effects, followed by model simplification (removal of model terms), and finally, complexification, with the addition of effects of spatial variation in climate and two-way interactions between terms. We validated diameter growth predictions from these models with independent observations, evaluating model performance in terms of accuracy, precision, and bias. We then compared predictions of future growth made by the existing large-tree diameter growth model used in FVS, i.e., without climate effects, to those of our updated models, including those with climate effects. We found that less complex models of tree growth outperform the current FVS model, and that the incorporation of climate effects improves model performance for two out of three species, in which predicted growth is greater than observed growth. Tree rings can be used to identify and incorporate drivers of growth variation into a

stand-level growth and yield model, giving more accurate predictions of the carbon uptake potential of forests under climate change.

1

Introduction

Though the combustion of fossil fuels since the Industrial Revolution has driven an increase in atmospheric carbon dioxide, this increase is not equal to the amount released by fossil fuel combustion. About half of anthropogenic emissions of carbon dioxide have been sequestered by the ocean and the terrestrial biosphere (Le Quéré et al., 2018). Of these two, the carbon sink of the terrestrial biosphere is less easily characterized and understood. By calculating the carbon flux of the atmosphere and ocean, it is estimated that the terrestrial biosphere removes from the atmosphere about one third of anthropogenic carbon emissions (Le Quéré et al., 2015). But because the factors and processes governing carbon sequestration by the terrestrial biosphere are not well characterized or understood, projections of the land uptake of carbon dioxide in the face of changing climate are uncertain (Friedlingstein et al., 2014). In particular, it is unknown whether terrestrial ecosystems will shift from being a carbon sink to a carbon source, the latter of which would lead to a destabilizing feedback on the climate system (Bonan, 2008).

Forests comprise one of the most important carbon pools in the terrestrial biosphere, and are estimated to account for a net global sink of 1.1 ± 0.8 Pg C year–1 (Pan et al., 2011). Simulation of forest response to changing conditions (e.g., climate) is key to be able to anticipate and influence (maintain and even enhance) the ecosystem services provided by forests, including carbon storage and sequestration. With advances in computational capacity, models of forest dynamics increasingly have the ability to represent the many processes that influence forest structure, composition, and function, such as climate variation and natural disturbances (Snell et al., 2014; Shifley et al., 2017; Albrich et al., 2020). These models can provide decade-scale predictions based on forest conditions and alternative scenarios, including management. However, models must accurately and precisely represent drivers

of forest change, particularly at a scale that is relevant to forest management, to be used to anticipate how much forests can contribute to climate repair. That is, validated models can be used to guide management decisions aimed at creating additional carbon sequestration and storage over long time scales, which is necessary for forests to act as a negative emissions pathway, as delineated under the Warsaw Framework on REDD+, or negative emissions technology, as described in a recent National Academies of Sciences, Engineering, and Medicine report National Academies of Sciences and Medicine (2019).

Forest growth and yield models that simulate forest dynamics at a stand scale have a long history of use in guiding management decisions, as well as advancement, by incorporating greater complexity to better represent forest dynamics (Weiskittel et al., 2011; Shifley et al., 2017). This lineage of forest models began with whole-stand models, dating back to the 1930's (MacKinney et al., 1937), followed by yield tables (Vuokila, 1965; Curtis, 1972) and differential growth equations (Buckman, 1962). These models were originally used to represent single-species, even-aged stands, i.e., plantations (García, 1984, 1994). The dynamics of uneven-aged forest stands were then addressed with forest models that simulate size-structured responses, such as matrix (Leslie, 1945; Usher, 1966, 1969; Buongiorno and Michie, 1980) and diameter-class (Ek, 1974; Hann, 1980) models. Subsequently, models that simulate tree-level responses to environmental conditions (Stage, 1973; Ek and Monserud, 1974; Wykoff et al., 1982) made it possible to capture the dynamics of both mixed-species (Porté and Bartelink, 2002) and uneven-aged (Peng, 2000) forest stands. Individual-tree growth and yield models have become the preferred method for forward projection of natural forest stand dynamics since the 1970s and 1980s. They have undergone extensive parameterization and validation to satisfactorily represent the competition-driven self-thinning process characteristic of closed-canopy forest stand development (Weiskittel et al., 2011).

The Forest Vegetation Simulator (FVS) is the forest growth and yield model most widely used in the United States (Dixon, 2002). FVS is an individual-tree model which uses tree and plot inventory data to simulate the growth, mortal-

ity, and response of a forest stand to silvicultural treatments, including thinning and prescribed fires (Crookston and Dixon, 2005). It is not spatially explicit; it is distance-independent. Further, it is an empirical model; the base models, such as growth, are parameterized or calibrated with regionally sourced data. There are 20 regional variants that are used to simulate silvicultural treatments, making the expected consequences of different management actions easy to compare in a multiple scenario framework, as required by the National Environmental Policy Act of 1969. Here, we focus on the growth component of FVS, specifically the diameter growth model, because it strongly influences stand development in simulations (Dixon, 2002), and it is a measure of carbon sequestration.

Only recently has it become possible to evaluate climate change impacts in FVS, with an extension called Climate-FVS (Crookston et al., 2010). Climate-FVS uses estimates of climatic suitability from species-level environmental envelopes (e.g., Rehfeldt et al. 2006) to modify forest dynamics, including tree-level growth. That is, climate responses are determined by modeling a species' occurrence data as a function of climate. This use of bioclimatic envelope models relies upon a series of hypotheses about the ecological niche (Hutchinson, 1957), and in particular about the relationships between environment, vital rates, population growth rate, abundance, and occurrence. The first, the abundant-center hypothesis, is that environmental conditions for a species are optimal at the center of its geographic range where abundance is also highest (Brown, 1984). Recognizing that abundance is a function of population growth rate, which is determined by underlying vital rates (i.e. birth, growth, mortality), a related hypothesis is the central-marginal or central-periphery hypothesis, which predicts that demographic performance, including individual growth, should decrease from the niche optimum to its edge (Maguire Jr, 1973; Hutchinson, 1978). However, these hypotheses are not widely supported; a recent review found little evidence that demographic performance decreases at range edges (Pironon et al., 2016). Instead, evidence has accumulated that the climate optimum for occurrence or abundance is frequently not the same as the optimum for underlying vital rates like growth (McGill, 2012; Thuiller et al., 2014; Pironon

et al., 2018; Bohner and Diez, 2019; Pagel et al., 2020). Hence, occurrence data may be a misleading way to anticipate how tree growth should respond to shifting climate.

Further, this species-level approach also does not account for variation in climate response across a species' geographical distribution or across environmental gradients, of which there is abundant evidence from forestry provenance trials (Langlet, 1971; Aitken and Bemmels, 2016). Climate-FVS can also be used to modify tree growth as a function of changing climate based on population-level climate responses estimated from such provenance tests (Leites et al., 2012), which are ideal for separating genetic vs. plastic responses (Alberto et al., 2013; Housset et al., 2018). However, these response functions are based on the cumulative growth of trees a certain number of years after they were planted, in response to the climate they experience in the common garden location (Leites et al., 2012). Therefore, the climate response estimated is average growth in response to average climate, and how that varies with provenance. Further, while there is a long history of forestry provenance trials(Langlet, 1971), there is a small number of species with suitable provenance data. Therefore, Climate-FVS applies the climate responses of a few species to others using two categories of climatic niche breadth (specialist vs. generalist; Crookston et al. 2010). This is a coarse representation of population-level responses to average climate conditions.

An alternative approach to model the effect of climate variation on individual tree growth is to use the response to climate variability recorded in annual growth rings ((Martin-Benito et al., 2011)). Tree rings sampled over a broad spatial scale can be used to quantify intraspecific (population-level) heterogeneity in average growth rate and the sensitivity of growth to interannual climate variability (McCullough et al., 2017; Canham et al., 2018; Klesse et al., 2020). That is, tree rings offer an empirical way to estimate species-specific responses to temporal and spatial variability in climate. Tree cores are collected easily and without harm to the tree with an increment borer, a tool that was invented by a forester with both practical and scientific intent, i.e., to explore environmental influences on tree growth (Somerville,

1891). However, this original intent has been far from fully realized. In forestry, the use of tree-ring data has largely been limited to estimating recent 5- or 10-yr diameter increment, as well as stand age. In dendrochronology, or more specifically dendroclimatology, tree-ring data have been used to reconstruct past climate, and in doing so, information on tree and stand conditions are removed through standardization, or detrending. That is, foresters have not fully utilized the information in annually resolved growth rings, in particular the climate response (Park Williams et al., 2013; Babst et al., 2017, 2019; Dannenberg et al., 2019), while dendrochronologists have focused on the climate response, but in terms of the relative rather than absolute width of growth rings. We fill this gap by using the information contained in absolute ring-widths on an individual tree's response to interannual variation in climate, tree, and stand conditions to incorporate climate-sensitivities into the FVS. This update offers an important path forward for forest growth and yield models to improve understanding of tree growth and hence prediction of how tree growth will respond to climate change, including how climate responses might interact with other drivers of variation in absolute tree growth.

Indeed, tree growth is understood to be a complex process. This is acknowledged by dendrochronologists in the form of Cook's aggregate model of tree growth (Cook, 1985), in which growth is a function of climate-related variability, tree age or size, the endogenous forest process of self-limiting growth (e.g. competition), and exogenous disturbances (e.g. fire or insect spread). In FVS, this complexity is addressed by including many predictors of tree growth, which we group into three categories: tree-level characteristics (size and vigor), site-level biophysical variables, and competition variables. However, including many predictors does not necessarily lead to more accurate predictions of growth (Pokharel and Froese, 2008). We use this opportunity to not only refit the diameter growth model in FVS with tree rings and add climate effects, but also consider species-specific structural changes to the representation of the process of tree growth. Specifically, we reexamine which predictors are needed to best predict tree growth. Is the current model structure overly complex by including uninformative predictors, e.g. collinear terms, or does it fail to capture important

complexity by not including certain effects, e.g. interaction terms?

Thus our aim is to build a climate-sensitive and parsimonious version of the large-tree diameter growth model currently used in FVS, based on tree-ring and forest inventory data. With this goal in mind, we designed a suite of alternative models to (1) test the effect of using tree rings to model growth on an annual time step (annualization); (2) test the effect of adding interannual climate variation as a predictor of growth variation; (3) test simpler models of the drivers of growth variation, eliminating terms currently used in FVS's large-tree diameter growth model, and finally (4) test for complexity (spatial heterogeneity, interaction effects) beyond what is currently considered by FVS. With this suite of alternative models, we ask: 1) does the use of tree-ring data improve model performance in terms of the accuracy (root mean square error, RMSE), precision (adjusted R2), and bias (slope) of growth predictions compared to out-of-sample observations? 2) What are the important drivers of growth variation estimated from tree-ring and forest inventory data? 3) How do predictions of future growth with improved growth models differ from predictions based on the base FVS model without climate effects? At each stage, we explore species-specific improvements upon the FVS growth model in terms of model performance and understanding of the drivers of tree growth.

2

Materials and Methods

2.1 Growth and Yield Model

Of the Interior West regional variants of FVS, we chose the Utah variant (Keyser and Dixon, 2019) as a testing framework for the incorporation of tree-rings into FVS, because it is well calibrated (DeRose et al., 2017). In the Utah variant, large-tree (>3 inches) diameter growth model is a multiple regression with the following functional form:

$$\begin{aligned} ln(dds) = {} & b1 + (b2 * SI) + (b3 * sin(ASP\text{–}0.7854) * SL) \\ & + (b4 * cos(ASP\text{–}0.7854) * SL) + (b5 * SL) \\ & + ((b6 * SL^2) + b7 * ln(DBH)) \\ & + (b8 * (BAL/100)) + (b9 * CR) + (b10 * CR^2) \\ & + (b11 * DBH^2) + (b12 * PCCF) + (b13 * (CCF/100)) \end{aligned} \tag{2.1}$$

Where dds is 10-year predicted change in squared inside-bark diameter (inches^2) (Dixon, 2002), and b are the estimated effects of each predictor (regression coefficients), with b1 an adjustment based on forest location (FVS_LOC_CD), and b2 an adjustment based on the dominant species in the stand. The covariates in this model fall into three categories. First are site-level biophysical variables, including slope (SL), aspect (ASP) and site index (SICOND). The terms sin(ASP–0.7854)* SL and cos(ASP–0.7854)* SL describe solar radiation by eastness and northness, respectively. SICOND is a measure of site quality, and represents the biomass production potential (Monserud, 1984). Second are variables concerning tree-level attributes: tree size (diameter at breast height, DBH) and a metric of tree vigor, crown ratio (CR). Third are variables capturing the competitive environment, either relative

to the focal tree (total basal area of live trees larger than the focal tree, BAL), of nearest neighbors (crown competition factor on a subplot, PCCF), or of the entire stand (crown competition factor on a plot, CCF). Each of these covariates is listed in Table 2.1 with a description, units, and their source (either obtained or calculated). The species-specific growth models used in the Utah variant of the FVS (Eq. 2.1) were originally based on the Prognosis model (Wykoff et al., 1982), and have since been updated as more data have become available (Keyser and Dixon, 2019).

Table 2.1: Covariates in the base FVS large-tree diameter growth model (Keyser and Dixon, 2019), with description and the source, either obtained from the FIADB (Burrill et al., 2018) or calculated, for each.

Acronym	**Name**	**Description**	**Source**
DBH	Diameter at breast height	Bole measured in inches at 1.3 m above ground	FIADB Tree Table
CR	Compacted crown ratio	Percentage (0 - 100) of the height of a tree with live foliage	FIADB TREE Table; change is calculated using the Weibull distribution (Dixon, 1985)
SI	Site index	Average height in feet the site species (SISP) is expected to attain in well-stocked, even-aged stands at a specified base age (SIBASE)	FIADB Condition Table
SL	Slope angle	To the nearest 1 percent	FIADB Condition Table

ASP	Aspect	To the nearest 1 degree	FIADB Condition Table
PCCF	Crown competition factor on the subplot	Measure of relative competition on the subplot expressed as percentage per acre	Calculated as the summation of individual tree crown competition factor (Krajicek et al., 1961; Keyser and Dixon, 2019)
CCF	Stand crown competition factor	Measure of relative competition expressed as percentage per acre	Calculated as the summation of individual tree crown competition factor (Krajicek et al., 1961; Keyser and Dixon, 2019)
BAL	Basal area of trees larger than the subject tree	Measure of absolute competition from above in square feet per acre	Calculated from DBH
SDI	Stand density index	Measure of stand stocking, trees per acre at a 25 cm DBH index	Calculated using the summation method (Stage, 1968; Shaw, 2000)

2.2 Data

We recalibrated the large-tree diameter growth model using tree- and plot-level data obtained from the Forest Inventory and Analysis database (FIADB; Burrill et al.

2018). The FIA program was mandated in 1928 with the goal of collecting data to characterize the status and trends of forested lands in the U.S., and hence its sampling was designed to be representative of the range of forest conditions in each state. Inventories were conducted periodically on a state-by-state basis until the passage of the 1998 Farm Bill, which mandated a standardized sampling approach and annual data collection nationwide. That is, trees are sampled based on a nationally standard fixed area radius plot design and a subset (10 - 20 percent) of plots in each state are inventoried every year, leading to more consistent data collection across the U.S under the annualized design. Under the periodic design, sampling approaches varied, including both fixed-radius and variable-radius plot designs. A point-based sample using a variable radius prism selects sample trees according to their size and distance from the sampling point. Trees used in calibrating models were collected during periodic inventories before 1999, mostly between 1988 and 1995, while model validation and projection of future growth were conducted with FIA data collected after 1999. The distribution of tree size for each data set ranged from 3 to over 30 inches (Figure 2.1).

Increment cores sampled in FIA's network of permanent sample plots throughout the interior western United States before 2000 were recently discovered and compiled into a tree-ring data network (DeRose et al., 2017). Although tree-ring data from the open-access International Tree Ring Data Bank (ITRDB) are widely used for dendrochronology studies, analyses of the sensitivity of tree growth to climate variability comparing data from the ITRDB against these FIA tree-ring data showed that climate sensitivities are systematically higher when estimated from the ITRDB, suggesting that targeted sampling of climate-sensitive trees makes this database biased (Klesse et al., 2018). The unbiased FIA tree-ring data set, both in terms of tree and stand conditions, presents a unique opportunity to use the rich information on climate effects recorded in annual growth rings, complemented by inventory data from their associated forest plots, to parameterize FVS growth models.

Increment cores collected on FIA plots were taken from tree species with a majority representation on the plot in terms of relative density, or stocking (Arner

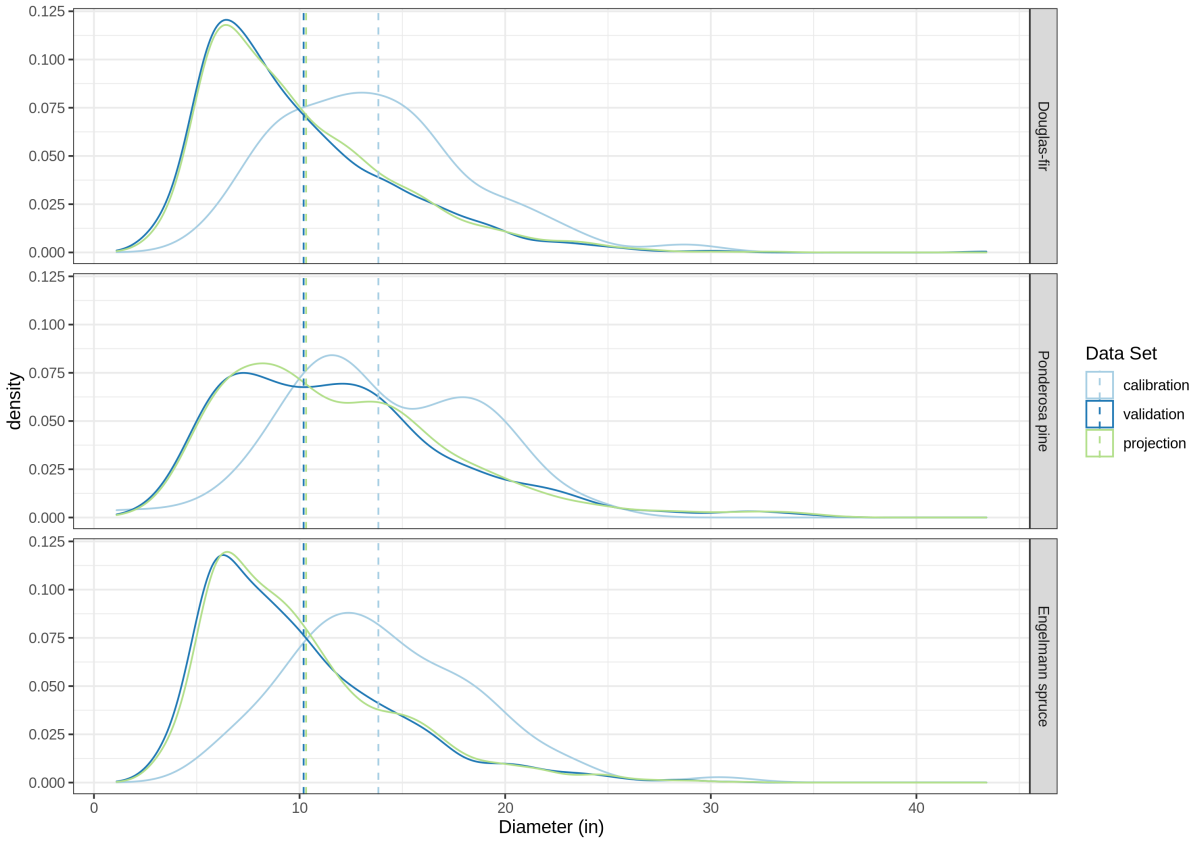

Figure 2.1: Diameter at breast height (DBH) distribution of the data used for calibrating (parameterizing) models, validating models, and using models to project future growth. Vertical dashed line represents the mean DBH.

et al., 2001). The information in these cores was originally used in the calculation of 10-year diameter increment and site index (DeRose et al., 2017). The ring-width time series data used here were developed from these increment cores by repreparing the samples, crossdating, and measuring ring widths according to standard dendrochronology protocol (Speer, 2010), as described in (DeRose et al., 2017). In particular, the process of crossdating is essential to assign and verify the year of growth ring formation (Black et al., 2016). These ring-width time series data were joined with their associated FIA plot data through a tree code that uniquely represents an individual tree in a given measurement year and location.

We used tree-ring and forest inventory data to parameterize species-specific growth models for the three most abundant tree species in both the tree-ring data network and in Utah forests, Douglas-fir (*Pseudotsuga menziesii* var. *glauca* Franco) (n = 111), ponderosa pine (*Pinus ponderosa* Lawson & C. Lawson) (n = 69), and Engelmann spruce (*Picea engelmannii* Parry ex. Engelm.) (n = 85), which provided a greater sample size to estimate effects. These species encompass the full elevational gradient of montane forests, which is positively correlated with precipitation and negatively correlated with temperature (Figure 2.2). Engelmann spruce occurs at high elevations and is the most shade tolerant, followed by Douglas-fir and ponderosa pine, respectively. Douglas-fir has the widest elevational range; this species can be found in low elevation canyons and on high elevation south-facing slopes. The distribution of sampled trees is evenly dispersed across Utah forested land with the exception of the drought tolerant ponderosa pine, which is concentrated in the southern region of Utah. Similarly to the evelational correlation, the latitudinal gradient is negatively correlated with temperature. Thus, climate effects associated with latitudinal and elevational gradients influence these species distributions

Climate data at 4-km resolution were downloaded from the PRISM Climate Group (Daly et al., 2008). Historical (1895-1980) and recent (1981-present) monthly total precipitation (mm), minimum average temperature (°C), and maximum average temperature (°C) were obtained from January 1985 to May 2020. Mean annual precipitation and mean annual temperature (°C) covering the period 1981 to 2010

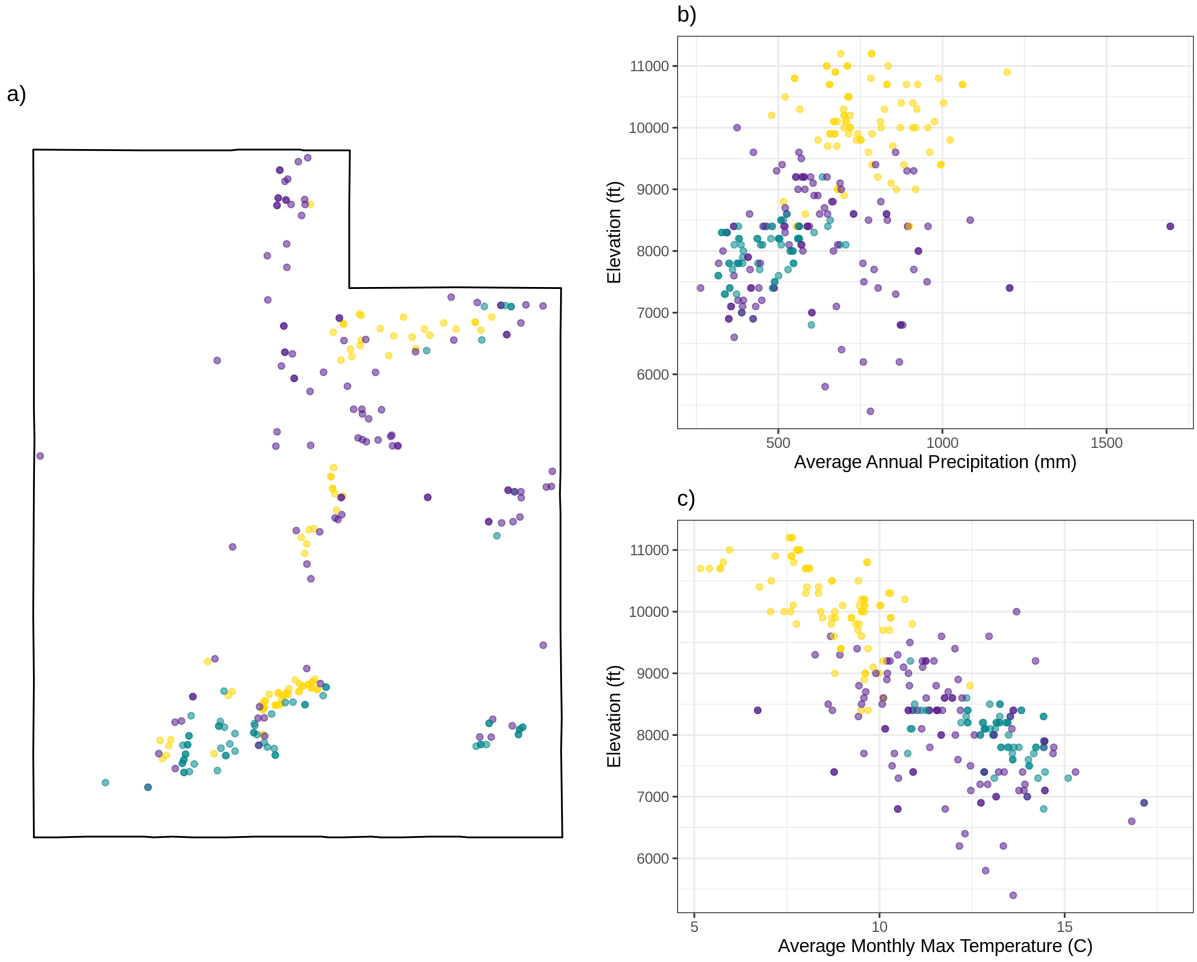

Figure 2.2: The distribution of trees from the calibration data set across the US state of Utah (a) as well as the average annual precipitation in millimeters (b) and monthly maximum temperature in degrees Celsius (c) experienced by each tree since 1960 in relation to its elevation in feet.

were obtained as climate normals, representing average climate conditions. We used the online archive of Downscaled CMIP3 and CMIP5 Climate and Hydrology Projections to obtain future climate from an ensemble of CMIP5 climate models. Specifically, we downloaded the BCSD-CMIP5-Hydrology projections of monthly precipitation (mm) and maximum temperature (°C) at $\frac{1}{8}$ degree resolution (approximately 12 km by 12 km) for all available climate models and representative concentration pathways (RCP) (Reclamation, 2014). Climate data were extracted using FIA plot-level latitude and longitude coordinates. To protect forest landowners, latitude and longitude coordinates that are available to the public are truncated, or 'fuzzed,' but are assumed to be within one kilometer of actual locations (Tinkham et al., 2018). Coordinate fuzzing has been shown to not affect species-level climate correlations (Gibson et al., 2014), although it may obscure fine-scale correlations with terrain attributes (Prisley et al., 2009).

2.3 Calibration

2.3.1 Annualization of focal tree size using tree rings

The first step towards incorporating climate data into the large-tree diameter growth model was the annualization of the data used to calibrate the model - that is, converting the time step the model operates on from ten years to one year - starting with the size (DBH) of trees from which increment cores were collected. DBH was obtained for the year of measurement from the FIADB (Table 2.1) and back-calculated using the ring-width data for each of these trees. To calculate DBH of the previous year, diameter increment (two times the width of the annual growth ring), adjusted by a species-specific bark growth factor (Keyser and Dixon, 2019), was subtracted from the DBH measurement (Dixon, 2002). This process was repeated to back-calculate DBH each year for 30 years or until the first year of ring-width measurements, whichever came first. We truncated tree-ring time series at a maximum of 30 years prior to the measurement year (going backwards in time). We chose this threshold as a compromise between maximizing the information on climate re-

sponses and minimizing the increasing uncertainty associated with reconstructing past forest conditions, such as the competitive environment (sometimes known as the "fading record"; Swetnam et al. 1999).

2.3.2 Back-calculation of time-varying predictors of growth

In order to back-calculate dynamic (time-varying) tree- and site-level predictors of tree growth for each year, annual DBH was needed for every tree on a plot, including trees that were not sampled for tree rings. Trees without increment cores, which contribute to the competitive environment by their presence on the plot, are referred to as "non-focal" trees. To back-calculate DBH for non-focal trees, we applied the basal area ratio (BAR) method used by FVS to impute missing diameter measurements (Dixon, 2002). We estimated annual basal area ratio change specific to our dataset by calculating BAR for each pair of years for each tree with an increment core.

$$BAR = DBH_0^2 / DBH_1^2 \tag{2.2}$$

We then assigned an average BAR to each non-focal tree, first based on matching plot and species, then species, and finally, an average across all plots and species. Average BAR was then used to back-calculate DBH every year for non-focal trees.

$$DBH_0 = \sqrt{BAR * DBH_1^2} \tag{2.3}$$

Once we obtained back-calculated values of DBH for non-focal trees, we annualized the competition variables that depend on the number and size of trees on a plot or subplot, which included BAL, PCCF and CCF (defined in Table 2.1). In addition, we calculated time-varying stand density index (SDI) using the summation method (Stage, 1968; Shaw, 2000). That is, stand density was calculated as the summation of individual tree diameters rather than an expansion of an average-sized tree (Reineke, 1933).

Which trees were included in the calculation of BAL, PCCF, CCF, and SDI depended on the sampling design. Most trees in the calibration data set were sampled on plots using a variable-radius design. Consistent with this variable-radius design, we calculated the distance from the sampling point for which a tree would be included in the sample, or limiting distance, which is based on its back-calculated DBH and the plot-specific basal area factor (BAF; Burrill et al. 2018). If the distance of the tree from the sampling point was larger than the limiting distance, that tree was dropped from the data set. The expansion factor, trees per acre (TPA), which is used to scale competition variables to a per-acre basis, was also updated annually based on DBH (Burrill et al., 2018). On fixed-radius plots, all trees were retained and TPA was assumed to remain constant over time.

A final step in the back-calculation of the competitive environment was to explicitly account for recently dead trees. To account for past competition from these trees, we included recently dead trees, under the assumption they had died in the 10 years before plot measurement (US Department of Agriculture, 2020). These trees were randomly assigned a mortality year from zero to 9 years prior to the measurement year and included in the calculation of competition metrics in the years prior to their death.

Compacted crown ratio (CR), the percentage of the total height of a tree with live foliage (Burrill et al., 2018), should change over time as a tree increases in height and the surrounding competitive environment changes. CR was extracted from the FIADB (Table 2.1) for the measurement year and back-calculated using the Weibull distribution method described by Dixon (1985). CR change was constrained to one percent per year, as it is in FVS, to avoid large changes (Keyser and Dixon, 2019).

2.3.3 Time-invariant predictors of growth

We treated slope (SL), aspect (ASP), and (SICOND) as constant over time. We also fit growth models with CR treated as constant, because we found poor correspondence between forward-calculated CR and observations of CR from inventories after 1999. Values of these time-invariant variables were obtained directly from the

FIADB (Table 2.1) for the measurement year (Burrill et al., 2018) for each tree and repeated for each year of growth.

2.3.4 Calculation of tree growth

We calculated annual dds (in2) from ring width (RW) observations in mm using (Dixon, 2002; Stage, 1973):

$$dds = (dib + (2 * (RW * 0.0393701)))^2 - dib^2 \tag{2.4}$$

Where dib is inside bark diameter at the beginning of the growth interval.

Missing values in the calibration data set were either corrected or the observation was removed. Missing rings (RW = 0, dds = 0) were replaced with the smallest ring-width measurement for that tree, to avoid taking the log of zero in regression models and as an alternative to choosing an arbitrarily small number to add to all observations. Site index was corrected when site species (SISP) associated with the site index on the condition (SICOND) did not match the species of the tree being modeled. This correction was done by cross matching plots from the periodic to annual design and extracting the appropriate site index (SICOND) for the species.

2.3.5 Model building - a series of tests

We fit a series of regression models of tree growth to systematically test whether updates to the current FVS large-tree diameter growth model (Eq. 2.1) improve model inference and prediction. The first was parameterized using the tree-ring data without modeling the effect of interannual climate variation on diameter growth, but including all terms in Eq. 2.1 (full annual), whereas the second also included the direct effect of climate (full climate). Hence the former tested the effect of annualizing growth with tree rings, while the latter tested the effect of incorporating climate sensitivities recorded in tree-rings. We then tested models of reduced complexity through stepwise removal of non-significant terms in Eq. 2.1 (reduced annual and reduced climate) to assess if all the terms in Eq. 2.1 are useful for predicting

annual growth. Finally, we added complexity to the reduced model versions, including spatial variation in climate normals (climate normals), and two-way interactions (normals + interactions) between model terms. As in the large-tree diameter growth model currently used in FVS (Eq. 2.1), all the models we built are multiple linear regressions that predict tree growth as a function of covariates (Tables 3.1, 3.2, and 3.3). We first describe details of these multiple regression models that were common across all model versions, followed by details about the model versions.

The response variable in the regression was log-transformed to correct for right skew. Although a generalized linear (mixed) model with a gamma distribution and a log link is often used to satisfy the assumption of normality for positive, right-skewed data, we used a linear (mixed) modeling of log-transformed dds to ease integration of model output into the FVS. In addition, residual analysis showed no improvement in a model with a gamma distribution and log link. Covariates were standardized by mean-centering and dividing by standard deviation, which facilitates model convergence and allows model coefficients to be interpreted as standardized effect sizes (Schielzeth, 2010). In order to standardize DBH and compare its effect against other predictors, we did not log-transform DBH (diverging from Eq. 2.1).

To account for correlation or clustering within the data set, we used linear mixed effects models, implemented in the R package lme4 Bates et al. (2015). Random effects reflect different possible patterns of correlation (or pseudoreplication) in the data. A random tree effect (tree-specific modification of the model intercept) was tested to account for variation among trees in average growth rate (dds); a random year effect (also an intercept modification) tested for systematic variation in growth rate among years not accounted for by climate predictors. Tree random effects were not nested within plot random effects because there was little to no replication of trees sampled for tree rings per plot. Tree random effects nested within forest location random effects were tested as an analog of the location intercept adjustment in the current FVS model (b1 in Eq. 2.1). We tested random effect structures with likelihood ratio tests, where the null hypothesis is that the simpler model is adequate. Model fit was further assessed for fixed effects using Akaike information criterion

(AIC; Akaike 1974).

These mixed effects models take the general form:

$$Y = X\beta + Zu + \epsilon \tag{2.5}$$

Where, Y is a vector of responses (ln(dds)), X is a matrix of predictor variables (covariates, Tables 3.1, 3.2, and 3.3), β is a vector of the fixed-effects regression coefficients (Figures 3.2, 3.4, and 3.6), Z is a matrix of the random effects and groups (DBH, tree, year), u is vector of the random effects, and ϵ is a vector of residuals.

2.3.6 Model versions

Compared to the annualized, tree-ring based model that was as similar as possible to Eq. 2.1 (full annual), the first set of species-specific model versions differ by including climate data (full climate). For each species, we identified monthly and seasonal precipitation and temperature variables that significantly influenced growth using response function analyses in the R packages dplR (Bunn, 2008) and treeclim (Zang and Biondi, 2015). Our strategy for selecting climate variables differed between precipitation and temperature. Because of high uncertainty among climate models with respect to projected future precipitation, we preferred the use of precipitation variables covering a longer rather than a shorter time window. While preliminary analyses indicated seasonal precipitation variables had higher correlations with ring-width variability and inclusion of these terms yielded lower AIC scores in regressions, we chose to use as a predictor in the diameter growth model total precipitation over a 16-month period for all species, with the idea that this may make predictions of future growth more robust in the face of changes in the timing of precipitation. Specifically, we chose a 16-month period that included the previous and current growing season, from previous June to current September, to account for significant lagged climate effects. In contrast, projected future temperature has

lower uncertainty, so we chose to use the monthly or seasonal temperature variables that most strongly correlated with ring-width index and gave the lowest AIC.

We then created reduced versions of these two groups of full-complexity models, to test whether simpler growth models might improve model performance (reduced annual and reduced climate). We eliminated covariates based on a lack of significance at the p=0.05 level (R package lmerTest; Kuznetsova et al. 2017) and patterns of collinearity determined by Variance Inflation Factor (VIF) with a threshold of 3 (R package car, Fox and Weisberg 2019), since the inclusion of multiple, collinear predictors can make model inference unstable (Dormann et al., 2013). We retained at least one competition covariate based on AIC score, even if it was insignificant at the p=0.05 level, because we considered the density-dependent regulation of growth necessary to capture forest stand development. In addition to the three competition variables in Eq. 2.1 (BAL, PCCF, and CCF), we tested stand density index (SDI) as a fourth alternative predictor. We also tested potential incoming solar radiation (from the R package solrad; Seyednasrollah 2018), as an alternative to the northness and eastness terms in Eq. 2.1 that combine aspect and slope. Finally, models with constant crown ratio were tested. Based on AIC score, several reduced model versions for each species were chosen to test in validation. However, for ponderosa pine, it was difficult to estimate effects given a small sample size, so we further tested statistically non-significant predictors, including site index and slope, and required the sign of the single competition coefficient retained to be negative, i.e., to match an a priori understanding of how forest stand development proceeds.

After reducing the number of terms in growth models, we then explored models with added complexity. First, we added climate normals to examine whether spatial variation in mean annual precipitation and mean temperature affect growth (climate normals). This model also included two-way interactions between climate normals and the time-varying climate predictors, to evaluate possible spatial variation in climate sensitivity caused by climate normals. Second, we included all two-way interactions (normals + interactions). The final forms of reduced and climate normal models were chosen after checking model performance through validation.

2.4 Validation

We performed out-of-sample validation (Cawrse et al., 2010) of diameter growth by comparing observed growth against predicted growth in trees independent of the calibration data. Trees used in validation were selected from the FIADB based on the following criteria: they had to be alive at two sequential measurements, larger at the remeasurement, and on forested plots with just one forest condition. Under these criteria, Douglas-fir (n = 891), ponderosa pine (n = 384), and Engelmann spruce (n = 1144) trees selected for validation were from the annualized (post-2000) design, which has a standardized fixed-radius sample design. Therefore, the expansion factor (in terms of TPA) was kept constant, unlike in the calibration data set where most plots had a variable-radius design.

All covariate data were obtained or calculated following the procedures used to create the calibration data set, except DBH of nonfocal trees. Here, as in calibration, nonfocal trees are other trees on a plot that constitute the competitive environment for a focal tree. Linear interpolation between the first and second measurement was used to annualize DBH of non-focal trees. If a tree died between the two measurements, diameter was linearly interpolated between the first measurement and the estimated year of death (given by the FIA variable MORTYEAR).

Growth of all focal trees was simulated from the initial measurement year to the remeasurement year using the alternative species-specific models created from the calibration data, including models listed in Tables 3.1, 3.2, and 3.3. That is, DBH of focal trees was calculated by adding to the initial measurement of DBH the diameter growth derived from model-predicted change in squared inside bark diameter (dds). Only fixed effects were used in predicting dds. We also validated the reduced models with various combinations of a radiation covariate (generated from solrad) and slope that gave the lowest AIC score in calibration, as well as a time-varying crown ratio vs. constant crown ratio.

We compared model-predicted diameter growth against observed diameter growth, i.e., the difference in DBH between inventory measurements (approximately

10-yr diameter increment), for all the tree-ring based model versions described above as well as the current FVS large-tree diameter growth model, which we established as a baseline for model performance. Model performance was quantified using three metrics derived from a regression of observed (on the y axis) vs. predicted (on the x axis) (Piñeiro et al., 2008) diameter increment: adjusted R squared (R^2), root mean square error (RMSE), and slope of the linear model. In these comparisons between observed vs. predicted growth, higher performing models had a slope closer to one, a higher value of R^2, and a lower value of RMSE. We chose a subset of the models that produced optimal values of these performance metrics for the next step, projection of tree growth under climate change.

2.5 Projection

Trees selected from the FIADB for projection of tree growth included Douglas-fir (n = 995), ponderosa pine (n = 460), and Engelmann spruce (n = 1340) in Utah from the most recent inventory, measured in 2010 or after, and were alive and on forested plots with just one condition. Trees with missing information that could not be corrected were removed from the projection exercise.

Growth of validation trees was projected using four high-performing annualized growth models: a model parameterized with tree-ring data and simplified based on the significance of effects (reduced annual), this reduced model with time-varying climate added as a predictor (reduced climate), followed by the previous model with climate normals added (climate normals), and finally climate normals and two-way interactions (normals + interactions). We stopped growth projections at 2060 due to the computational toll of repeated projection cycles. All covariates were obtained from FIADB or calculated as in validation, except the DBH of non-focal trees and climate data. Growth of non-focal trees was projected with FVS using 5-year projection cycles, then annualized using linear interpolation. Projections in the Utah variant of FVS included mortality, which is distributed across the expansion factor (TPA) of each tree in a stand. Because of tree mortality, TPA was updated

every year by linearly interpolating TPA output from FVS. In the models that include climate as a predictor of growth, PRISM data were used for years before 2020, whereas beginning with the year 2020 (and after), downscaled projections of future climate (Reclamation, 2014) were used. In total, models that included the effect of climate (reduced climate, climate normals, normals + interactions) were used to project tree growth using output from 50 different combinations of general circulation model (GCM) and emissions scenario: 21 GCM projections under the "green world" scenario of RCP2.6 and 29 GCM projections under the "business as usual" scenario of RCP8.5 (see Table A1).

We then used two methods to compare relative growth rate predicted by four updated growth models - reduced annual, reduced climate, climate normals, and normals + interactions - against growth predicted by the current FVS large-tree diameter growth model. Relative growth rate is calculated as the change in DBH divided by the size of the tree (DBH) at the beginning of the growth projection period. The first comparison was a paired-sample t-test to estimate the mean difference in cumulative growth to 2060 for each growth model, GCM, and RCP combination. Second, to examine differences in relative growth rate related to tree size, we used a paired sample t-test to estimate the mean difference in cumulative growth to 2060 for seven 5-inch diameter classes from 3 to 38 inches for each growth model, GCM, and RCP combination. In both methods, we filtered for significant differences (p ¡ 0.05) and further calculated the average difference for each emissions scenario (RCP2.6 or RCP8.5) for models with climate effects (reduced climate, climate normals, or normals + interactions). Values above zero indicate the updated growth model predicted more growth than the current FVS model, whereas values below zero indicate that the updated growth model predicts less growth than FVS.

3

Results

3.1 Calibration

For each species, likelihood ratio tests failed to reject models with a random intercept for each year and a random effect for each tree on the model intercept (average dds) and the effect of diameter on dds ($p < 0.001$). That is, the adequacy of models with a simpler random effect structure was rejected, and the addition of a random intercept for each tree nested within a forest (FVS_LOC_CD), which is analogous to FVS's use of forest location code to modify average growth, did not consistently improve model fit to data across species.

Response function analyses revealed that precipitation was most strongly correlated with ring-width index, especially previous summer and current summer precipitation across species (Figures 3.1, 3.3, and 3.5). The temperature covariate that resulted in the lowest AIC score was average maximum temperature summarized from February to July for Douglas-fir, average maximum temperature from June to August for ponderosa pine, and average maximum temperature of the previous August for Engelmann spruce.

Collinearity among covariates was limited (VIF <3.0); hence, none were dropped for this reason. Instead, we kept covariates in reduced-complexity models (Tables 3.1, 3.2, and 3.3) based on statistical significance (alpha = 0.05) for explaining variation in growth and performance in validation. Competition covariates (BAL, CCF, PCCF, SDI) did not consistently explain variation in growth across species. While the current FVS large diameter growth model includes more than one competition parameter for each species-specific model, we kept one competition variable for each species-specific model in models annualized with tree-ring data, which was sufficient to explain the negative effect of competition. We dropped the northness and east-

ness radiation terms because their effects were not significant and were inconsistent across species.

With standardized covariates across models, effect sizes were based on the magnitude of the coefficient (Schielzeth, 2010). In all models, DBH had the largest effect on diameter growth (Figures 3.2, 3.4, and 3.6). A positive effect of the linear term and a negative effect of the quadratic term indicated that at the smallest DBH values, diameter increment increases with increasing DBH, whereas at larger values of DBH, diameter increment declines with increasing DBH. This is consistent with the current species-specific models of FVS that include both the linear and quadratic effect of DBH. After DBH, the next-largest effects in the reduced models of Douglas-fir and Engelmann spruce were crown ratio, site index, and slope (Figs. 1 and 3). The effects of crown ratio and site index were positive, as in FVS's current large tree diameter growth model. The effect of slope was consistently negative when growth was modeled on the basis of tree-ring data, whereas in the current large tree diameter growth model, the effect of slope varies in sign (positive vs. negative) across species. In the reduced model of ponderosa pine growth, the effects of site index and slope were of similar magnitude compared to the effects of interannual precipitation and temperature (Figure 3.4), whereas in reduced models of Douglas-fir and Engelmann spruce growth, interannual precipitation and temperature had smaller effects than site index and slope (Figures 3.2 and 3.6). Across all three species, the effect of precipitation on growth was positive, whereas the effect of temperature was negative, as expected. In addition, the interaction between interannual precipitation and temperature was positive, implying that a higher value of one resulted in a greater, more positive effect of the other. Variables describing competitive pressure (BAL, CCF, SDI) had the smallest effect on diameter growth for all species (Figures 3.2, 3.4, and 3.6). While interannual climate and competition had small effect sizes, they also had the smallest standard error estimates, indicating high confidence in those effects. In all three species, adding climate normals to the growth model made the interaction between interannual precipitation and temperature no longer significant.

3.1.1 Douglas-fir

Temperature normals significantly affected variation (across space) in growth, whereas precipitation normals did not (Figure 3.2). When climate normals were added to the growth model, temperature normals became the largest, positive climate effect. The interaction between interannual precipitation and precipitation normals and the interaction between interannual temperature and precipitation normals was significant, which indicated significant spatial variation in the climate-sensitivity of Douglas-fir growth. The former was a negative effect, implying that at higher average precipitation there was less positive effect of precipitation on growth, while the latter was a positive effect, implying that at higher average precipitation there was a less negative effect of temperature on growth. The interaction of SDI with both precipitation variables (interannual precipitation and precipitation normals) was significant. The interaction with interannual precipitation was positive, implying that at high stand density there was a more positive effect of interannual precipitation on growth, while the interaction with precipitation normals was negative, implying that at higher average precipitation there was a more negative effect of competition on growth.

3.1.2 Ponderosa pine

Precipitation and temperature normals did not themselves explain variation in ponderosa pine growth, but interactions between climate normals and other variables did significantly explain growth variation, including the interaction between interannual precipitation and both precipitation and temperature normals, as well as the interaction between BAL and precipitation normal (Figure 3.4). As with Douglas-fir, the interaction between interannual precipitation and precipitation normal was negative, while the interaction between interannual precipitation and temperature normal was positive, implying that at higher average temperature there was a more positive effect of precipitation on growth. The interaction between BAL and precipitation normal was negative, implying that at high average precipitation there was

Table 3.1: Covariates of Douglas-fir models, including the current species-specific FVS large tree diameter growth model (current fvs), a model parameterized with tree rings that best matches the previous model (full annual), a model that adds the effect of time-varying climate (full climate), and a model reduced based on the significance of effects (reduced annual and reduced climate), with (+) indicating a positive sign and (-) a negative sign on the coefficient estimate.

parameter	Current FVS	Annual Full	Climate Full	Annual Reduced	Climate Reduced
DBH	+	+	+	+	+
DBH2	0	−	−	−	−
CR	+	+	+	+	+
CR2	−	+	+	0	0
SI	+	+	+	+	+
SL	−	−	−	−	−
SL2	−	−	−	0	0
sin(ASP*0.7854)*SL	+	+	+	0	0
cos(ASP*0.7854)*SL	+	−	−	0	0
PCCF	−	−	−	0	0
CCF	0	0	0	0	0
BAL	−	−	−	0	0
SDI	0	0	0	−	−
Precip	0	0	+	0	+
Temp	0	0	−	0	−
Precip:Temp	0	0	+	0	+

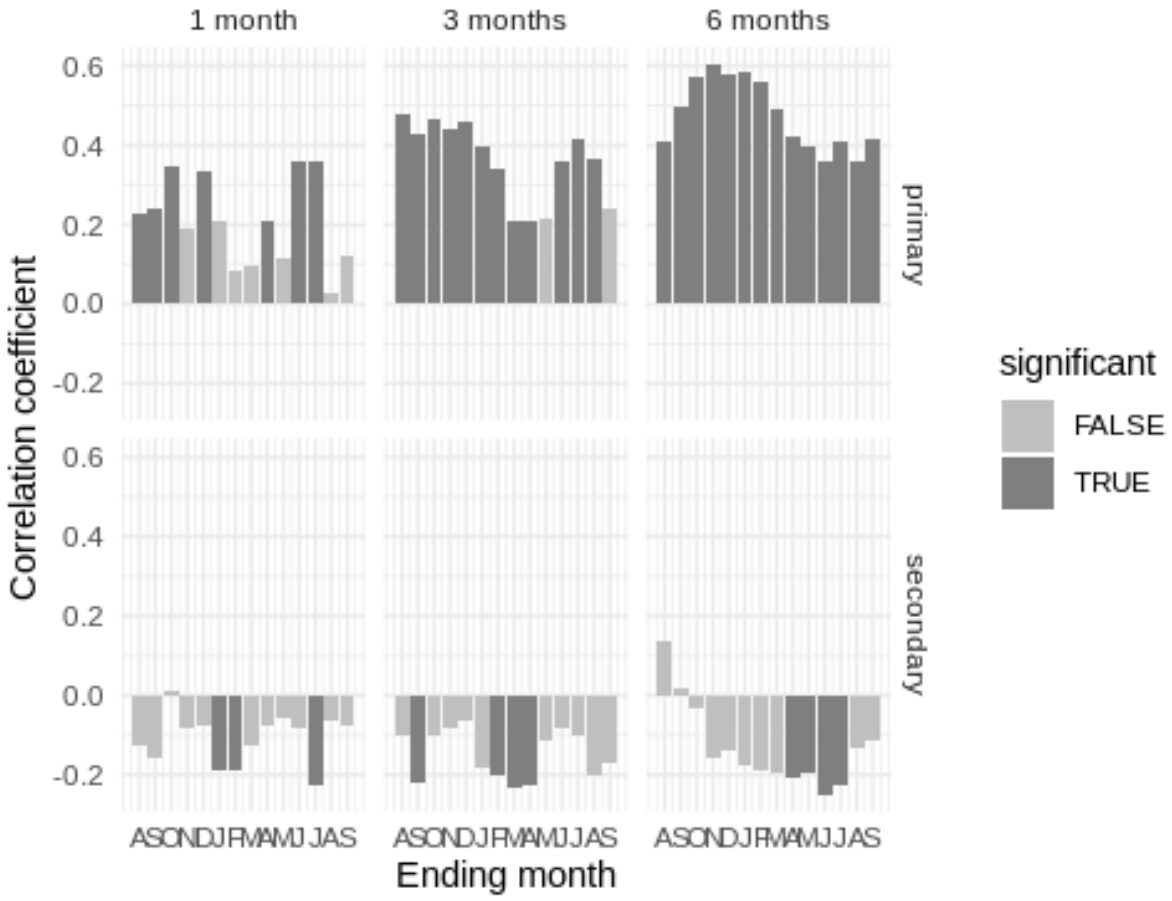

Figure 3.1: Monthly and seasonal (3 and 6 month) precipitation (primary) and temperature (secondary) correlations with Douglas-fir ring width index.

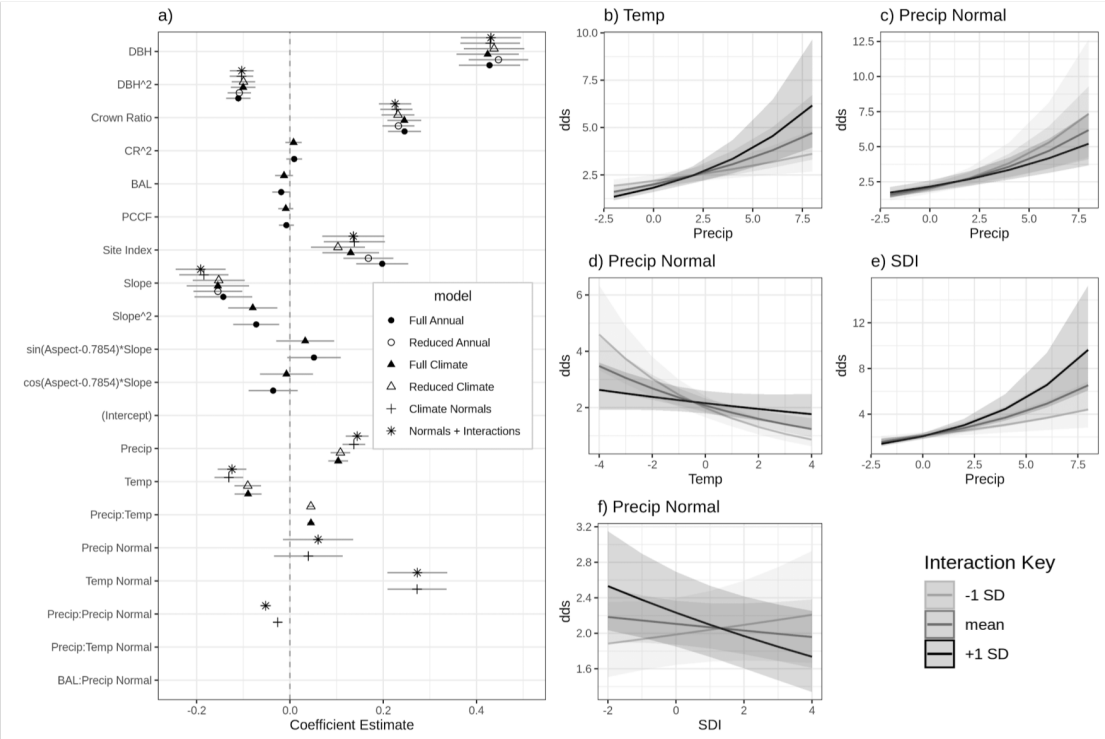

Figure 3.2: Estimates of standardized coefficients and their standard errors for Douglas-fir growth models, including a model parameterized with tree rings that best matches the current species-specific FVS large tree diameter growth model (full annual), a model that adds the effect of time-varying climate (full climate), and a model reduced based on the significance of effects (reduced annual and reduced climate). Also included are models which add complexity, such as climate normals (climate normals) and two-way interactions (normals + interactions). Marginal effects of interaction terms on dds are plotted, including time-varying precipitation and time-varying temperature, time-varying precipitation and precipitation normal, time-varying temperature and precipitation normal, time-varying precipitation and stand density index, and stand density index and precipitation normal. These plots show one main effect (on the x axis) conditional on levels of the other main effect, being the mean and one standard deviation above and below the mean.

Table 3.2: Covariates of ponderosa pine models, including the current species-specific FVS large tree diameter growth model (current fvs), a model parameterized with tree rings that best matches the previous model (full annual), a model that adds the effect of time-varying climate (full climate), and a model reduced based on the significance of effects (reduced annual and reduced climate), with (+) indicating a positive sign and (-) a negative sign on the coefficient estimate.

parameter	Current FVS	Annual Full	Climate Full	Annual Reduced	Climate Reduced
DBH	+	+	+	+	+
DBH2	−	−	−	−	−
CR	+	−	+	0	0
CR2	+	−	−	0	0
SI	+	+	+	+	+
SL	+	−	−	−	−
SL2	+	−	−	0	0
sin(ASP*0.7854)*SL	−	−	−	0	0
cos(ASP*0.7854)*SL	−	+	+	0	0
PCCF	−	+	+	0	0
CCF	0	0	0	0	0
BAL	−	−	−	−	−
SDI	0	0	0	0	0
Precip	0	0	+	0	+
Temp	0	0	−	0	−
Precip:Temp	0	0	+	0	+

a more negative effect of competition on growth.

3.1.3 Engelmann spruce

Climate normals did not significantly explain growth variability, but the interactions between interannual precipitation and both precipitation normal and temperature normal were significant, as well as the interaction between interannual temperature and temperature normal and between the competition variable BAL and interannual precipitation (Figure 3.6). As with ponderosa pine, the interaction between interannual precipitation and precipitation normal was negative, and the interaction between interannual precipitation and temperature normal was positive. The

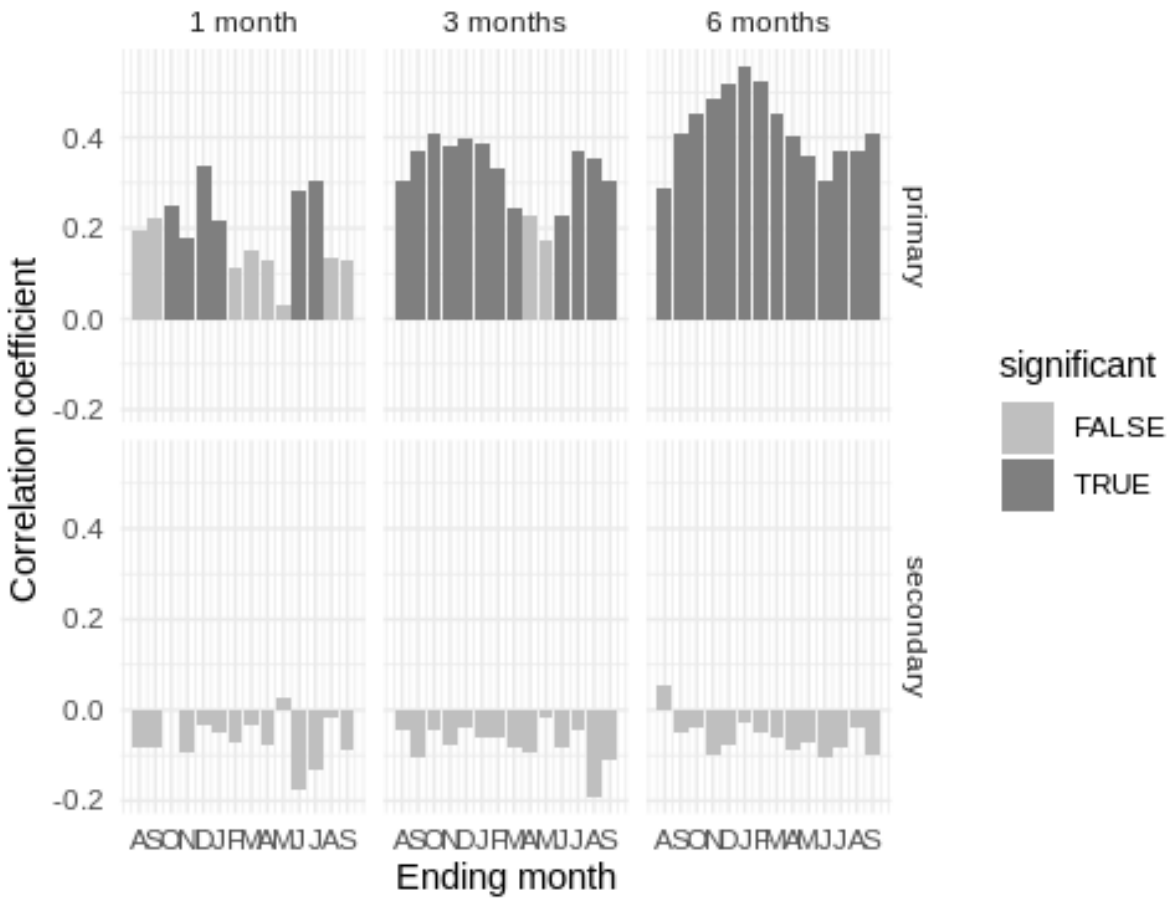

Figure 3.3: Monthly and seasonal (3 and 6 month) precipitation (primary) and temperature (secondary) correlations with ponderosa pine ring width index.

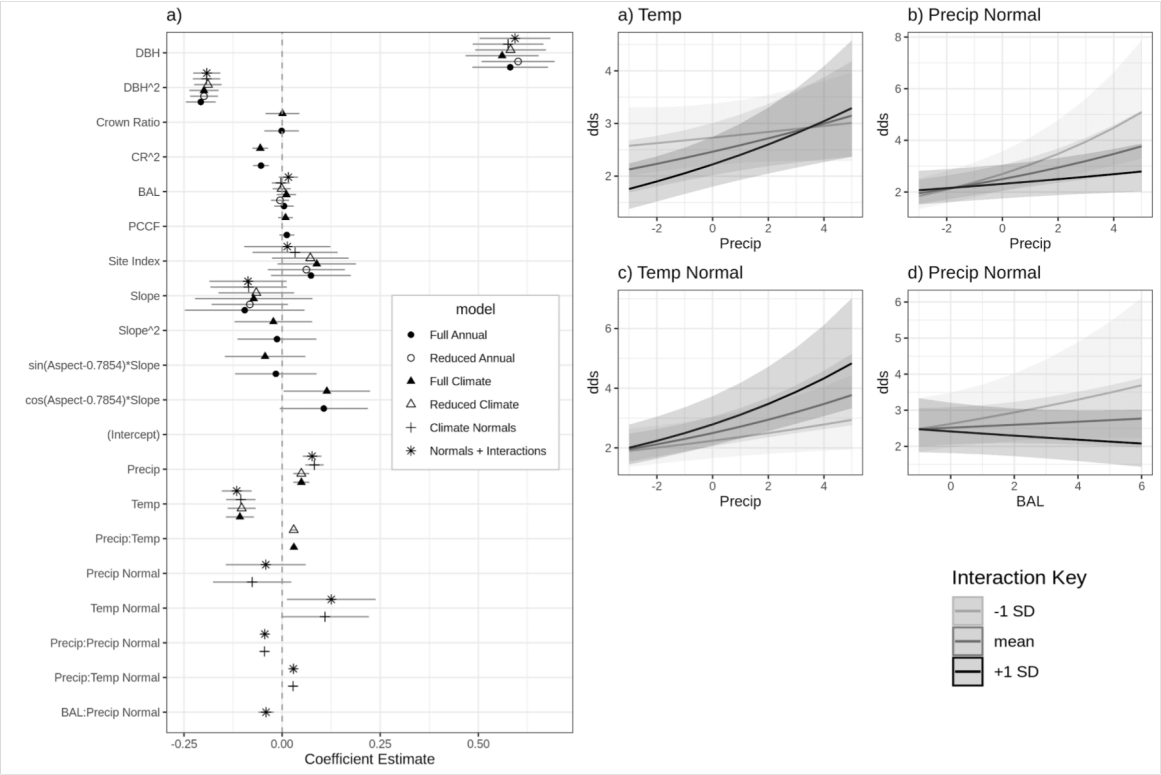

Figure 3.4: Estimates of standardized coefficients and their standard errors for ponderosa pine growth models, including a model parameterized with tree rings that is as similar as possible (in the terms included) to the current species-specific FVS large tree diameter growth (full annual), a model that adds the effect of time-varying climate (full climate), and a model reduced based on the significance of effects (reduced annual and reduced climate). Also included are models which add complexity, such as climate normals (climate normals) and two-way interactions (normals + interactions). Marginal effects of interaction terms on dds are plotted, including time-varying precipitation and time-varying temperature, time-varying precipitation and precipitation normal, time-varying precipitation and temperature normal, and BAL and precipitation normal. These plots show one main effect (on the x axis) conditional on levels of the other main effect, being the mean and one standard deviation above and below the mean.

Table 3.3: Covariates of Engelmann spruce models, including the current species-specific FVS large tree diameter growth model (current fvs), a model parameterized with tree rings that best matches the previous model (full annual), a model that adds the effect of time-varying climate (full climate), and a model reduced based on the significance of effects (reduced annual and reduced climate), with (+) indicating a positive sign and (-) a negative sign on the coefficient estimate.

parameter	Current FVS	Annual Full	Climate Full	Annual Reduced	Climate Reduced
DBH	+	+	+	+	+
DBH2	0	−	−	−	−
CR	+	+	+	+	+
CR2	+	+	+	0	0
SI	+	+	+	+	+
SL	+	−	−	−	−
SL2	0	0	0	0	0
sin(ASP*0.7854)*SL	−	+	+	0	0
cos(ASP*0.7854)*SL	−	+	+	0	0
PCCF	0	0	0	0	0
CCF	−	+	+	0	0
BAL	−	−	−	−	−
SDI	0	0	0	0	0
Precip	0	0	+	0	+
Temp	0	0	−	0	−
Precip:Temp	0	0	+	0	+

interaction between interannual temperature and temperature normal was negative, implying that at higher average temperature there was a more negative effect of temperature on growth. Finally, the interaction between BAL and interannual precipitation was positive, implying that at higher levels of competition there was a more positive effect of precipitation on growth.

3.2 Validation

Across all species, the parameterization of growth models with tree-ring data improved performance compared to the baseline FVS large-tree diameter growth model

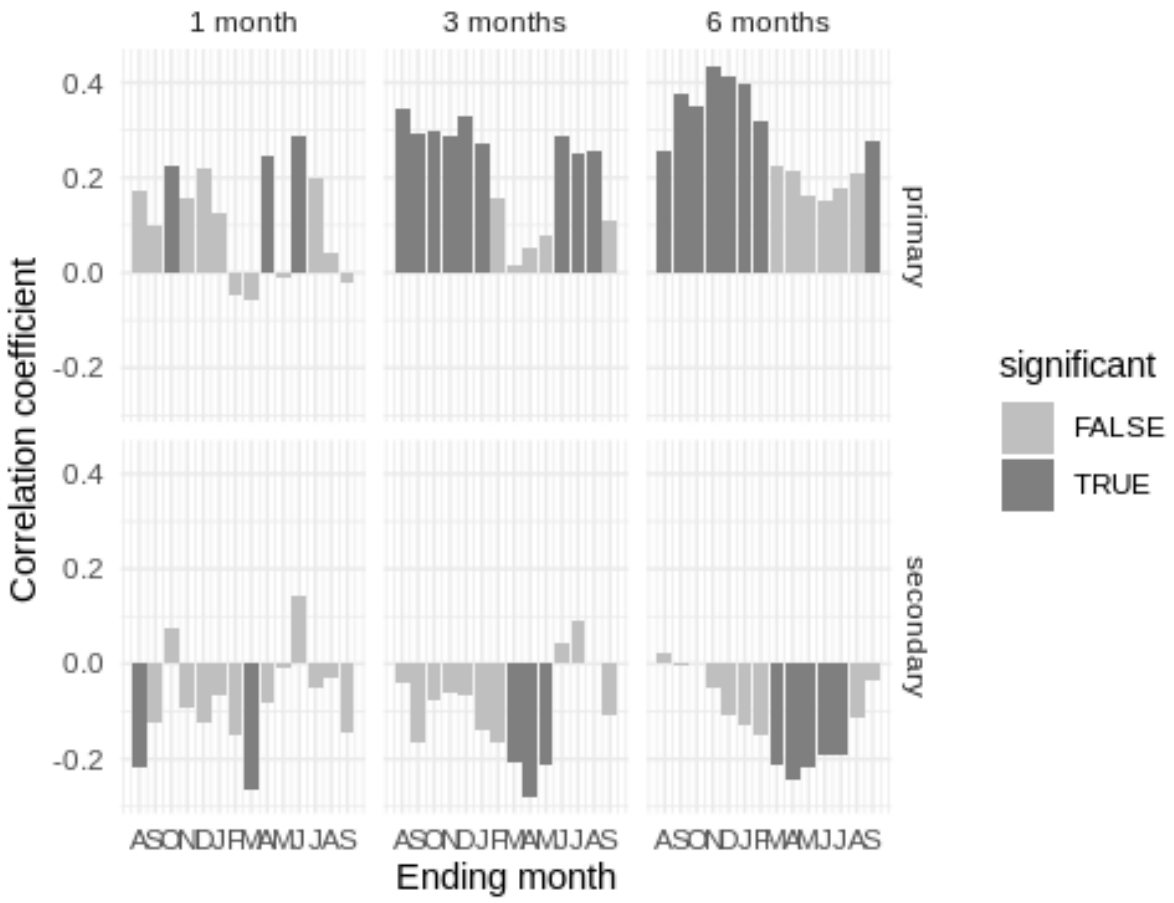

Figure 3.5: Monthly and seasonal (3 and 6 month) precipitation (primary) and temperature (secondary) correlations with Engelmann spruce ring width index.

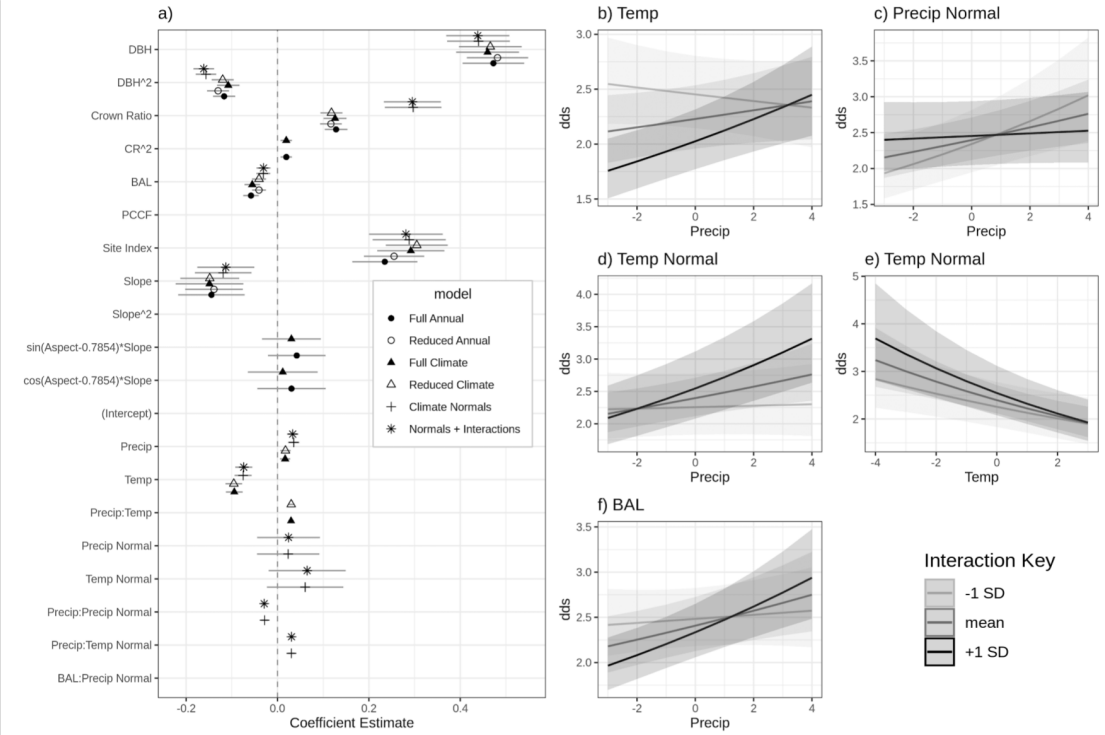

Figure 3.6: Estimates of standardized coefficients and their standard errors for Engelmann spruce growth models, including a model parameterized with tree rings that is as similar as possible (in the terms included) to the current species-specific FVS large tree diameter growth (full annual), a model that adds the effect of time-varying climate (full climate), and a model reduced based on the significance of effects (reduced annual and reduced climate). Also included are models which add complexity, such as climate normals (climate normals) and two-way interactions (normals + interactions). Marginal effects of interaction terms on dds are plotted, including time-varying precipitation and time-varying temperature, time-varying precipitation and precipitation normal, time-varying precipitation and temperature normal, time-varying temperature and temperature normal, and time-varying precipitation and BAL. These plots show one main effect (on the x axis) conditional on levels of the other main effect, being the mean and one standard deviation above and below the mean.

(Figure 3.7), in terms of adjusted R^2, RMSE, and slope of the regression of observed vs. predicted diameter growth increment. Among the models parameterized with tree-ring data, reduced models had higher performance across all three validation metrics than full models that included all the covariates in the current FVS model.

3.2.1 Douglas-fir

The reduced-complexity model parameterized with tree-ring data that did not include the effect of climate (reduced annual) performed the best by optimizing R^2, RMSE, and match between observed vs. predicted diameter growth increment (Figure 3.7). This was only a slight improvement on the baseline FVS large-tree diameter growth model. Indeed, the performance of the baseline FVS model was remarkably high for Douglas-fir (slope of 0.9277), compared to much poorer performance of the baseline FVS ponderosa pine and Engelmann spruce models (slopes of 0.1906 and 0.3978, respectively). Adding climate predictors to the Douglas-fir growth model lowered performance, in terms of slope, compared to the baseline FVS model. For the reduced model with climate normals, R^2 was higher and RMSE was lower than the baseline FVS model. Back-calculated CR outperformed constant CR as a metric of tree vigor.

3.2.2 Ponderosa pine

The reduced-complexity model with interannual climate performed the best (reduced climate), in terms of the match between predicted and observed diameter increment (slope = 0.5626) (Figure 3.7). The baseline FVS growth model had a lower root mean square error (0.5278) and a higher R^2 (0.0728) than this reduced climate model (RMSE of 0.5305 and R^2 of 0.0633), but its slope was much lower (0.1906). After the model with interannual climate, the reduced-complexity model that did not include climate (reduced annual) outperformed the reduced model with both interannual climate and climate normals (climate normals) and the reduced model with climate normals and interactions (normals + interactions). Although

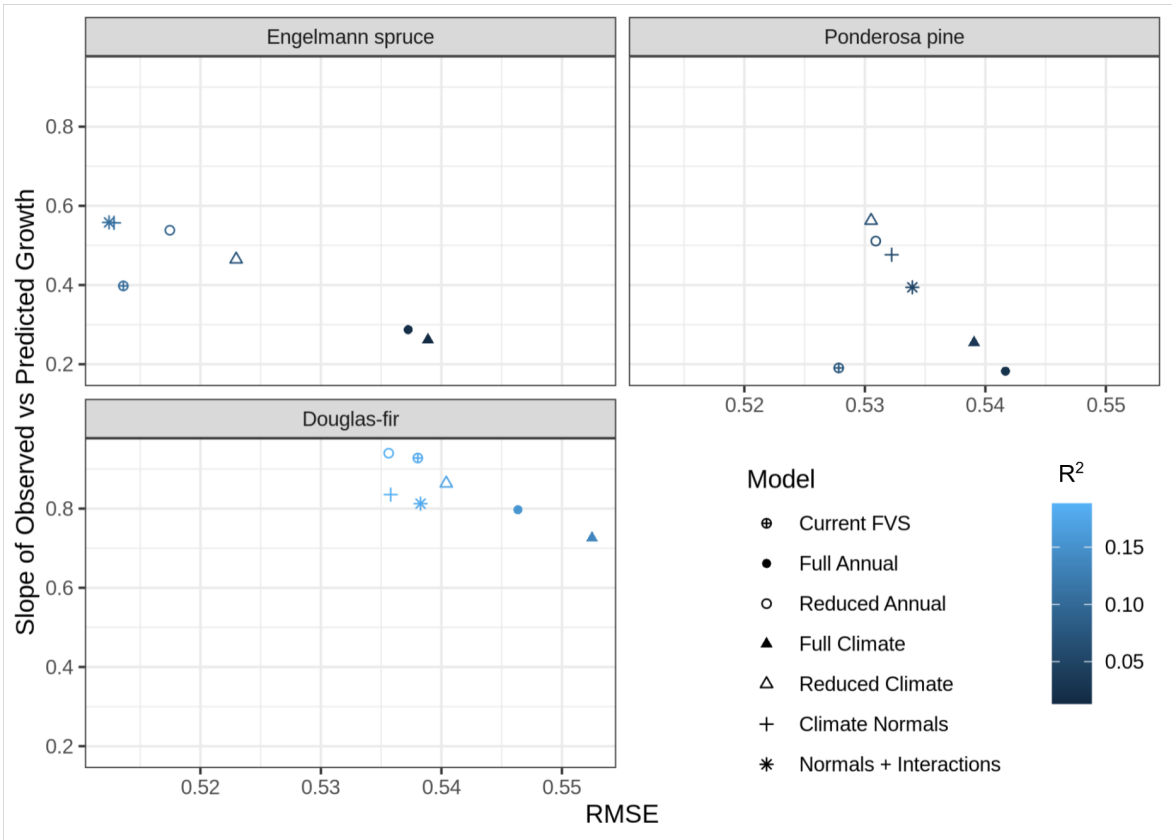

Figure 3.7: Comparison of model performance, in terms of adjusted R^2, root mean square error (RMSE), and slope of the linear regression of observed vs. predicted diameter growth increment, for all species-specific growth models (Douglas-fir, ponderosa pine, and Engelmann spruce). These include a large tree diameter growth model that is as similar as possible to the current growth model used in FVS, but parameterized with tree-ring data (full annual), a model that adds the effect of time-varying climate (full climate), and a model reduced based on the significance of effects (reduced annual and reduced climate). Also included are models which add complexity, such as climate normals (climate normals) and all two-way interactions (normals + interactions).

the site index and slope terms were insignificant (Figure 3.4), model performance improved with these included.

3.2.3 Engelmann spruce

The reduced model with climate normals and interactions performed the best by optimizing R^2, RMSE, and the match between predicted and observed diameter increment, which was comparable to the performance of the reduced model with climate normals (Figure 3.7). In terms of slope, the reduced-complexity model that did not include climate (reduced annual) and the reduced-complexity model with interannual climate (reduced climate) outperformed the baseline FVS growth model, but these models had a lower R^2 and higher RMSE. In these models, constant crown ratio outperformed back-calculated crown ratio.

3.3 Projection

Across all species, the reduced model parameterized with tree-ring data that does not include the effect of interannual climate (reduced annual) predicted greater relative growth rate from the measurement year to 2060 than the current FVS large-tree diameter growth model (Figures 3.8, 3.9, and 3.10). There were species-specific differences for selected models with the effect of climate, including the reduced-complexity model parameterized with tree-rings that includes the effect of interannual climate (reduced climate), the previous model with climate normals added (climate normals), and the previous model with two-way interactions added (normals + interactions). For Douglas-fir, these models all predicted more cumulative growth (Figure 3.8), but for ponderosa pine and Engelmann spruce, models with the effect of climate predicted less cumulative growth than the current FVS model (Figures 3.9 and 3.10). For Engelmann spruce, we found that models with the effect of climate normals (climate normals and normals + interactions) had less of a reduction in cumulative growth from the current FVS model than the reduced climate model (Figure 3.10), but for Douglas-fir and ponderosa pine, the differences between

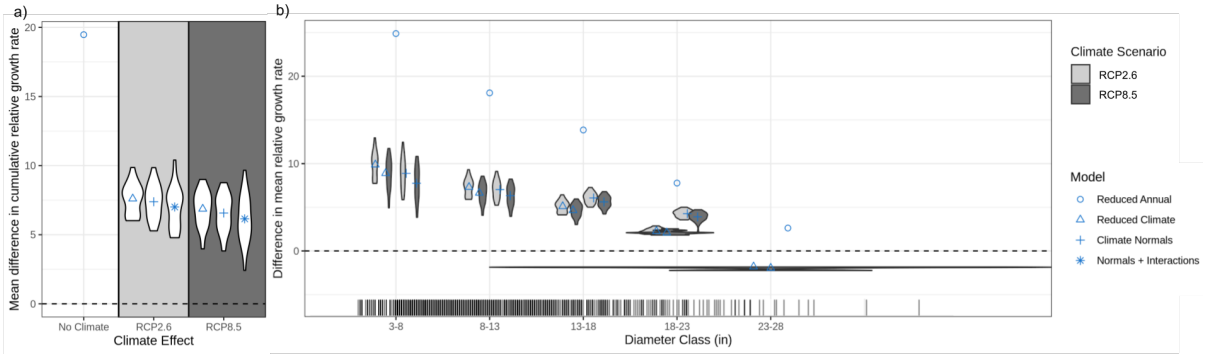

Figure 3.8: Average difference in relative growth rate based on initial tree size between Douglas-fir model variants (see Table 3.1) with no climate effect, a climate effect assuming a future scenario of RCP2.6, or a climate effect assuming a future scenario of RCP8.5 and the current FVS large tree diameter growth model cumulatively from measurement year to 2060 (a) and per 5 years from 2020 to 2060 for seven 5-inch diameter classes from 3 to 38 inches (b). Negative values indicate less predicted growth than the current FVS model, while positive values indicate more predicted growth. Variation in general circulation model climate projections (see Table A1) is given by the distribution around the mean and the rug shows the distribution of tree size at the start of the projection.

models were small (Figures 3.8 and 3.9). Across diameter classes, we found a greater difference in growth for lower diameter classes (Figures 3.8, 3.9, and 3.10). Finally, while the higher emission scenario, RCP8.5, on average predicted less growth than the lower emission scenario, RCP2.6, the difference was small (Figures 3.8, 3.9, and 3.10).

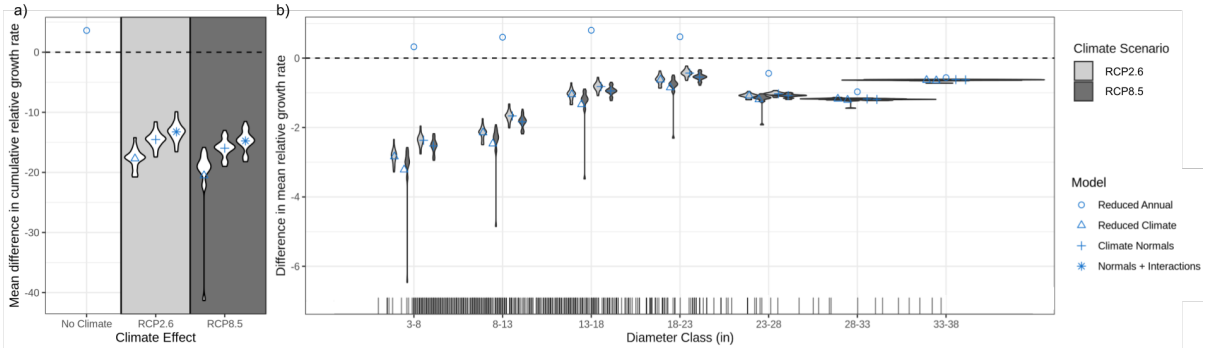

Figure 3.9: Average difference in relative growth rate based on initial tree size between ponderosa pine model variants (see Table 3.2) with no climate effect, a climate effect assuming a future scenario of RCP2.6, or a climate effect assuming a future scenario of RCP8.5 and the current FVS large tree diameter growth model cumulatively from measurement year to 2060 (a) and per 5 years from 2020 to 2060 for seven 5-inch diameter classes from 3 to 38 inches (b). Negative values indicate less predicted growth than the current FVS model, while positive values indicate more predicted growth. Variation in general circulation model climate projections (see Table A1) is given by the distribution around the mean and the rug shows the distribution of tree size at the start of the projection.

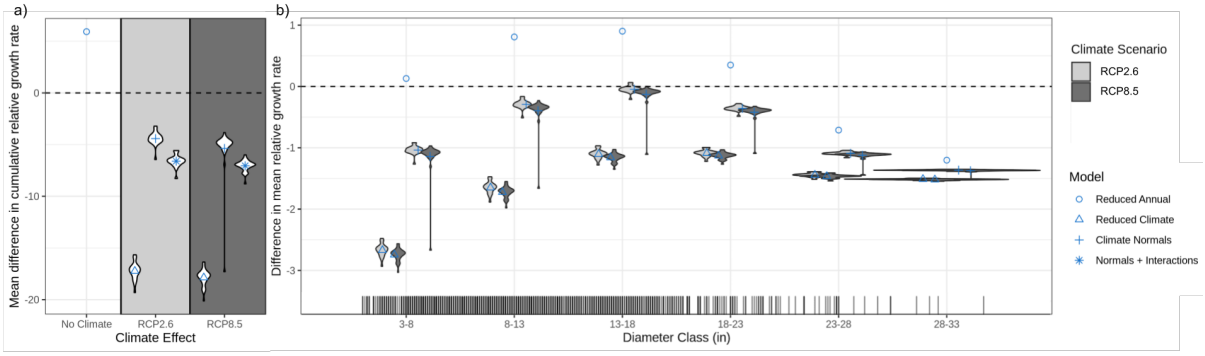

Figure 3.10: Average difference in relative growth rate based on initial tree size between Engelmann spruce model variants (see Table 3.3) with no climate effect, a climate effect assuming a future scenario of RCP2.6, or a climate effect assuming a future scenario of RCP8.5 and the current FVS large tree diameter growth model cumulatively from measurement year to 2060 (a) and per 5 years from 2020 to 2060 for seven 5-inch diameter classes from 3 to 38 inches (b). Negative values indicate less predicted growth than the current FVS model, while positive values indicate more predicted growth. Variation in general circulation model climate projections (see Table A1) is given by the distribution around the mean and the rug shows the distribution of tree size at the start of the projection.

4

Discussion

4.1 Improved prediction of tree growth with tree rings

Models parameterized with tree-rings and simplified by removing terms outperformed the current FVS large tree diameter growth model, suggesting that the current model is overly complex. The effects in the current FVS model have been tuned over time based on forestry expertise, but keeping all of these predictors in an annualized growth model led to poorer prediction. Instead, we suggest the annual-resolution information on tree growth in tree rings can be used to pare models down to a subset of terms that improve prediction in a given species and geographic area.

Beyond the consistent improvement of predictive performance with model simplification, which model performed best differed between species. Model performance was optimized using only tree-ring-based annualization for Douglas-fir, with the incorporation of temporally-varying climate effects for ponderosa pine, and with further model complexity by adding climate normals and two-way interactions for Engelmann spruce. Prediction of Douglas-fir growth by the current FVS model is already highly accurate and precise, such that adding climate effects did not improve prediction. In contrast, for ponderosa pine and Engelmann spruce, the incorporation of climate effects reduced bias in predicted diameter growth, which is overpredicted in the current FVS growth model. With the effect of climate change explicitly accounted for in ponderosa pine and Engelmann spruce, we can expect less growth on average than what is predicted by the current FVS model. Therefore, for species with low model performance in FVS, parameterization with tree rings yielded more accurate predictions of growth and the carbon uptake potential of trees under climate change.

4.2 Refined understanding of the drivers of tree growth variability

Along with improved predictive performance, we found that the use of tree-ring data helped to better represent the underlying drivers of tree growth, especially climate, and identify processes that could be better understood, such as competition. The current FVS model accounts for spatial variation in growth, some of which is caused by spatial variation in climate, through an adjustment to average growth based on a coarse location code that reflects U.S. Forest Service forest unit boundaries (Dixon, 2002). This adjustment leads to discrete shifts in predicted growth between location boundaries. We tested an analogous model parameterized with tree-ring data and found that these boundaries (in Utah) were unsupported by the data. In contrast, we have shown that tree rings can be used to incorporate the direct effects of temporal and spatial variability in climate on tree growth, including spatial variation in tree growth influenced by spatial variation in average climate, interannual variation in tree growth influenced by interannual variation in climate, and spatial variation in the sensitivity of tree growth to time-varying climate. The last of these, the addition of an interaction between climate normals and time-varying climate predictors, captures the hypothesis that variation in climate sensitivity may be caused by average climate conditions, as articulated by Fritts et al. (1965). Indeed, across species, we found increased climate sensitivities at dry and warm locations (lower than average precipitation and higher than average temperature for a given species) (Figures 3.1, 3.3, and 3.5). This is consistent with the idea that individual growth is soil moisture-limited across all three of these dominant tree species in Utah, from low to high elevation, and that climate sensitivity increases as climate becomes more limiting. Tree-ring data make it possible to capture this heterogeneity in climate response beyond what is provided by the current FVS growth model (location adjustment and regionally specific variants) and at higher temporal resolution than Climate-FVS (Crookston et al., 2010). With locally sourced tree-ring time series data, foresters can better characterize climate vulnerability and expected climate impacts specific to their management unit.

Climate-FVS addressed the assumption of climate stationarity by modifying expected growth with changing climate at the species or population level (Crookston et al., 2010). However, in addition to poor correspondence between climate responses based on species-level occurrence data vs. individual tree growth data, and a lack of provenance data to model species-specific population-level climate responses, it is difficult to see how this approach could estimate interactions between climate and other drivers of tree growth. By incorporating the direct effect of climate we were able to explicitly model interactions between climate and tree or stand characteristics. These interactions are particularly important because managers cannot manipulate climate, but they can influence some of the other drivers of tree growth that may interact with climate. For example, we found a significant interaction effect between climate and competition. Competition within the stand increases climate sensitivities, suggesting that forests can be managed (thinned) to mitigate climate vulnerability. In addition, we found spatial variation in the response to competition: trees in a drier region of their climatic range are less sensitive to the presence of other trees (Figures 3.1 and 3.3). The benefit of more or larger neighbors at these sites may reflect facilitation through microclimate effects. This pattern could also reflect an interaction between competition and site quality. Pretzsch and Biber (2010) found that the mechanism of competition moves from aboveground to belowground with decline in site quality. Other interactions that we tested, e.g., between tree size and time-varying climate predictors, explained variation in growth but did not lead to more accurate predictions. By explicitly modeling interactions we can consider additional complexity in the process of tree growth, but further exploration with more data, or ideally through experimentation, is needed to verify these effects. Indeed, overfitting to data can lead to poor extrapolation, and model complexity should be added with care.

In addition to this exploration of climate effects and interaction effects involving climate, parameterization with tree rings allowed us to critically examine other factors influencing tree growth. Some of the terms in the current FVS model, including tree size, site index, and slope, had consistent effects across species in our

updated models, and their inclusion was supported both by calibration and out-of-sample validation. However, across species, which predictor best captured the negative density-dependent regulation of competition varied. The calculations of competition predictors are designed to capture different competitive mechanisms. One-sided (asymmetric) competition variables, such as BAL, consider competition only from trees larger than the subject tree, with competition for light in mind, whereas two-sided (symmetric) competition parameters, such as CCF, PCCF, and SDI, consider competition from both sides of the diameter distribution relative to the subject tree, with competition for below-ground resources in mind, such as soil moisture and nutrients (Weiskittel et al., 2011). To capture both of these mechanisms, both categories of competition variables are often included in models of tree growth (Weiskittel et al., 2011). However, which type of competition variable best explains growth may depend on the ecology of the species. Canham et al. (2004) was able to separate the effect of aboveground and belowground competition experimentally and found that shade tolerant trees were more sensitive to crowding (two-sided) rather than shading (one-sided), supporting the idea that one-sided competition variables capture competition for light. But in our models, the competition predictors retained across species did not match cross-species patterns of shade tolerance. Growth in both the least shade-tolerant species, ponderosa pine, and the most shade-tolerant, Engelmann spruce, was best explained by a one-sided competition variable, BAL. How best to represent competition in these individual-tree growth and yield models remains a worthy area of investigation, as the process should be expected to vary, in mechanism and magnitude, across species limited by different resources or along environmental gradients.

We note that two of the drivers of growth variation included in our model - climate and competition - have small effects, and yet they are critical to anticipate how forests will behave under changing climate. While small, these effects are well constrained, and they accumulate over time. We found that in addition to the current FVS model, the reduced model parameterized with tree rings also predicts more cumulative growth than updated models with climate effects (Figures 3.8, 3.9,

and 3.10). With climate explicitly represented we find a reduction in future growth. Yet, through added complexity, we found that climate sensitivities can be modified by local adaptations and the competitive environment of the stand. In Engelmann spruce, projected reductions in growth due to sensitivity to interannual climate alone were buffered by accounting for spatial variation in climate sensitivity (Figure 3.10). A better understanding of these interactions can aid in management decisions which aim to maintain and enhance ecosystem services, including increased growth and carbon sequestration.

4.3 Opportunities for future improvement

Our work suggests several avenues for further improvement of a climate-sensitive growth model in the FVS. Inference from empirical models depends directly on the quantity and quality of the data used in calibration. For example, ponderosa pine had the smallest sample size of the three species modeled, in terms of the number of tree-ring time series available, and the drivers of ponderosa pine growth were not easy to identify. Tree size and climate effects were the only statistically significant predictors of growth during calibration, yet in validation, the addition of other predictors, site index (SICOND) and slope (SL), improved model performance. It seems possible that these statistically weak effects may reflect the limited sample size for ponderosa pine. Further, enhanced data on the right-hand side of growth equations, i.e., in the predictor variables, can also better constrain effects and improve understanding of the drivers of growth variation. Several ways in which shortcomings on the right-hand side of our growth equation can lead to poor prediction are by 1) not fully capturing the range of a driver in calibration, which can lead to extrapolation of effects, and poorly representing a driver by 2) imperfect estimation of unobserved drivers, i.e., through proxies or observable metrics or 3) inaccurate interpolation of time-varying predictors. In the following paragraphs we describe these issues of extrapolation, proxy metrics, and interpolation for each category of drivers in the growth models: climate-related, tree-level, competition, and site-level biophysical

variables. We offer solutions to resolve these issues moving forward.

4.3.1 Climate

While tree rings offer a way to empirically estimate climate sensitivities for many species, projection of future growth based on those climate sensitivities relies on tree responses to future climate being the same as their responses to past climate, an assumption known in dendrochronology as "uniformitarianism" (Fritts, 1976). Violating this assumption, growth responses have been found to have shifted with changing climate in the latter part of the 20th and early 21st centuries, e.g., from positive to negative sensitivity to temperature variability at high latitudes (Babst et al., 2019). If tree responses to climate are changing, a model may fit well to contemporary climate but extrapolate poorly to novel conditions (Evans, 2012). The addition of an interaction between climate normals and sensitivity to time-varying climate is one way to capture how the climate sensitivity of tree growth might vary across, for example, increasingly warmer average temperature. This approach relies on space-for-time substitution (Pickett, 1989), which assumes the past response of a tree in a warmer (on average) location can be projected (substituted) for a tree at a currently cooler location when it experiences a warmer future. However, this assumption is problematic as well (Klesse et al., 2020). While a tree core records the phenotypic plasticity of individual tree growth - a tree's response to interannual variability in climate - wild-sourced tree rings cannot determine to what degree average growth rate is genetically vs. plastically determined. Provenance data (or pedigree-free genomic analyses; K. Swartz, pers.comm) are needed to know how average growth will respond to changes in average climate conditions. For this reason, we did not apply future climate data to climate normals during projection of future growth, following the example of Klesse et al. (2020). A further point is that while the addition of climate normals to interannually-varying climate predictors, along with their interactions, explained more of the variation in the ring-width data, it did not consistently lead to increased model performance across species. A second possibility, in terms of addressing the problem of shifting climate sensitivities as

climate changes, is to estimate a nonlinear climate response, i.e., increased climate sensitivity as temperatures get warmer. Nonlinear responses can be modeled with a quadratic term on the time-varying climate predictors, or by using a GAM, spline, or other basis function. And a third possibility to solve the problem of shifting climate sensitivities is to take a process-based approach, i.e., incorporate outputs of a physiological model driven by climate. Milner et al. (2003) linked the physiological model STAND-BGC to FVS, but growth estimates do not account for local adaptation (Crookston et al., 2005). Tree-ring data can also be used to fit a function form of tree growth that is chosen based on a physiological understanding of growth (Tolwinski-Ward et al., 2011; Mina et al., 2016).

4.3.2 Tree characteristics

Consistent with other individual tree growth and yield models (Monserud and Sterba, 1996), we found tree-level predictors, tree size and crown ratio, to have the largest effect on diameter growth. Because of the magnitude of these effects, it is particularly important for calibration data to span the full range of these predictors. For example, the size distribution of trees sampled can bias estimated growth rates (Bowman et al., 2013). We had relatively little data on very large trees for calibration of the growth model (Figure 2.1), such that the effect of tree size on diameter growth is extrapolated at large values. Further, we note that the greatest contrast in predicted growth between our models vs. the current FVS model falls at the small tree size-class (Figures 3.8, 3.9, and 3.10). We suggest that data collection efforts should focus on broadening the diameter distribution by increasing the sample size of trees that are cored to include more small or young trees and large or old trees, so that size-related growth responses can be better constrained at small and very large tree sizes.

Crown ratio, a metric of tree vigor, significantly predicted annual growth in Douglas-fir and Engelmann spruce, but there are several indications that this covariate is problematic when estimated or interpolated. When testing simpler models, we found that the inclusion of crown ratio as a predictor did not consistently op-

timize model performance. In Douglas-fir, time-varying crown ratio outperformed constant crown ratio, while in Engelmann spruce, constant crown ratio outperformed time-varying crown ratio. These two approaches have been shown to generate very different predictions of growth (Leites et al., 2012). Further, we found that crown ratio change calculated with the Weibull distribution did not match observed values. In the case of ponderosa pine, we found that tree crown ratio did not significantly explain annual growth variability. Ponderosa pine is the least shade tolerant among the three species studied (followed by Douglas-fir and Engelmann spruce, respectively). Hence, crown ratio would be expected, a priori, to be an important predictor of its growth. As noted above, we had relatively little data for ponderosa pine (n = 69), so it may be that a lack of data made it difficult to detect an effect of crown ratio. We conclude that an improved method to calculate crown ratio change, along with more data, are needed to better capture the influence of tree vigor in an annualized growth model.

4.3.3 Competition

A persistent challenge in forest models is historical information on competitive conditions - the number and size of trees. Without repeated measurement of trees spanning decades (e.g., at experimental forests), the competitive environment must be back-calculated from a measurement year. This leads to error or uncertainty in competition covariates, which will inevitably increasingly diverge from the true, but unknown past forest stand structure (Swetnam et al., 1999). Tree rings offer a way to directly calculate attributes from tree- to stand-level for annual growth models, in contrast to the methods used by Cao (2000) and Weiskittel et al. (2007). However, for the competitive environment to be interpolated using this method, annually resolved growth is needed for every tree on the plot. Given that we only had about one increment core per forest plot, we assumed a constant rate of growth for trees without increment cores. To improve upon this and other methods for interpolation or estimation of annual stand density (Cao and Strub, 2008), we suggest the collection of increment cores from all trees per plot, to more precisely calculate

annual competition predictors.

4.3.4 Site-level biophysical variables

We treated the site-level biophysical variable site index as constant through time. However, site index is a purely phenomenological measure of site quality that depends on climate (Monserud et al., 2008) and can therefore be expected to change with climate, influencing expected growth. In Climate-FVS, site index change is modeled as a proportional change in climate suitability, which can modify expected growth (Crookston et al., 2010). We suggest instead to incorporate the mechanism which determines the height and age relationship modeled by site index, like we have done here by including the direct effect of climate on growth.

Solar radiation is an important driver of tree growth through its influence on land surface temperature, evapotranspiration rates, soil moisture, and hence the drought stress experienced by trees; however, we found the northness and eastness radiation variables in the current FVS growth model did not significantly explain growth in our models or produce better (more accurate) predictions of growth. A more refined estimate of radiation may better capture these effects. For example, high-resolution radiation information that accounts for topographic shading in addition to slope and aspect can be extracted from geographic information systems software (Hofierka and Suri, 2002), but to test these fine-scale effects, precise, unfuzzed coordinates of trees are required (Prisley et al., 2009).

Starting with these opportunities for improvement, a re-engineering of the large-tree diameter growth model, invoked by Pokharel and Froese (2008), could better capture the processes influencing tree growth. Unfortunately, terms representing processes known to be important drivers of growth did not always fit data well or led to poor prediction. This was due to issues of extrapolation, proxy metrics, and interpolation in our predictors, which can be addressed with more tree-ring data collected systematically on forest inventory plots (DeRose, Evans, et al. in prep) and improved calculations of predictors. Still, we recognize we may not have identified every opportunity for improvement for a diameter growth model parameterized with

tree rings.

4.4 Conclusions

This work demonstrates that tree rings can be used to improve upon the FVS large-tree diameter growth model, by including an important driver of tree growth (climate) and increasing predictive performance. The large-tree diameter growth model has a strong influence on the behavior of simulations in FVS (Dixon, 2002). Projected tree size is used to calculate other tree and stand attributes, feeding back on subsequent diameter growth predictions. Thus, the growth model is a crucial determinant of forest stand development. Without accounting for the effect of climate, FVS will make increasingly poor projections as climate changes. We improve upon earlier methods of incorporating climate effects into FVS (Milner et al., 2003; Crookston et al., 2005, 2010) by using tree rings to model the direct effect of interannual climate variability. These improvements continue a long history of updates to this stand-level growth and yield model (Dixon, 2002).

Thus we have addressed an important need in forest management in the U. S. - i.e., for a climate-sensitive version of the growth model at the heart of the Forest Vegetation Simulator. These improvements were made possible thanks to tree-ring data collected by the Interior West FIA program (DeRose et al., 2017). With this workflow developed for three species under the Utah variant of FVS and tree-ring data collected in other regions, locally parameterized climate-sensitive diameter growth models can be developed for other species in the other 19 variants of FVS across the U.S. Incoming inventory measurements of tree size, which are generated every year, can then be used to validate the projections of these climate-sensitive growth models, and further refine the representation of the process of tree growth. Indeed, these models serve as hypotheses about what influences tree growth and how. This annualized, climate-sensitive version of FVS lends itself to the practice of near-term iterative forecasting and adaptive management by foresters (Walters, 1986; Dietze et al., 2018). That is, after a management decision is put into action

based on a projection of forest vulnerability, incoming forest inventory measurements will provide observations from which to validate the model projections and adjust the model to further improve the understanding and prediction of tree growth.

However, to better represent forest systems in a nonstationary world, development of the FVS needs further investment. Forest managers are increasingly called upon to estimate the carbon consequences of management decisions, and stand-level models are well-suited to do so (Moore et al., 2012; Puhlick et al., 2020), yet they have fallen behind other forest models. We suggest improving upon this widely used forest growth and yield model so that managers can better anticipate the consequences of changing climate and manage to maintain and enhance forest ecosystem services, including carbon sequestration.

5

Appendix A - Future Climate Data

Table A1: Global circulation models and emission scenarios used to project future growth, adapted from technical memorandum by the Bureau of Reclamation (2014).

WCRP CMIP5 Climate Modeling Group	WCRP CMIP5 Climate Model ID	Emissions Scenarios	
		RCP2.6	RCP8.5
Commonwealth Scientific and Industrial Research Organization and Bureau of Meteorology, Australia	ACCESS1-0		X
Beijing Climate Center, China Meteorological Administration	BCC-CSM1-1	X	X
	BCC-CSM1-1-M		X
Canadian Centre for Climate Modelling and Analysis	CanESM2	X	X
National Center for Atmospheric Research	CCSM4	X	X
Community Earth System Model Contributors	CESM1-BGC		X
	CESM1-CAM5	X	X
Centro Euro-Mediterraneo per I Cambiamenti Climatici	CMCC-CM		X

Centre National de Recherches Météorologiques/Centre Européen de Recherche et Formation Avancée en Calcul Scientifique	CNRM-CM5		X
Commonwealth Scientific and Industrial Research Organization, Queensland Climate Change Centre of Excellence	CSIRO-Mk3-6-0	X	X
Laboratory of Numerical Modeling for Atmospheric Sciences and Geophysical Fluid Dynamics, Institute of Atmospheric Physics, Chinese Academy of Sciences, and Center for Earth System Science, Tsinghua University	FGOALS-g2	X	X
The First Institute of Oceanography, State Oceanic Administration, China	FIO-ESM	X	X
NOAA Geophysical Fluid Dynamics Laboratory	GFDL-CM3	X	X
	GFDL-ESM2G	X	X
	GFDL-ESM2M	X	X
NASA Goddard Institute for Space Studies	GISS-E2-H-CC		X
	GISS-E2-R	X	X

	GISS-E2-R-CC		X
Met Office Hadley Centre (additional HadGEM2-ES realizations contributed by Instituto Nacional de Pesquisas Espaciais)	HadGEM2-AO	X	X
	HadGEM2-CC		X
	HadGEM2-ES	X	X
Institute for Numerical Mathematics	INM-CM4		X
Institut Pierre-Simon Laplace	IPSL-CM5A-MR	X	X
	IPSL-CM5B-LR		X
Japan Agency for Marine-Earth Science and Technology, Atmosphere and Ocean Research Institute (The University of Tokyo), and National Institute for Environmental Studies	MIROC-ESM	X	X
	MIROC-ESM-CHEM	X	X
Atmosphere and Ocean Research Institute (The University of Tokyo), National Institute for Environmental Studies, and Japan Agency for Marine-Earth Science and Technology	MIROC5	X	X
Max-Planck-Institut für Meteorologie (Max Planck Institute for Meteorology)	MPI-ESM-LR	X	X
	MPI-ESM-MR	X	X

Meteorological Research Institute	MRI-CGCM3	X	X
Norwegian Climate Centre	NorESM1-M	X	X

REFERENCES

Aitken, S. N. and J. B. Bemmels (2016). Time to get moving: assisted gene flow of forest trees. *Evolutionary Applications*, **9**(1). ISSN 1752-4571. doi:10.1111/eva.12293.

Akaike, H. (1974). A new look at the statistical model identification. *IEEE Transactions on Automatic Control*, **19**(6). ISSN 0018-9286. doi:10.1109/TAC.1974.1100705.

Alberto, F. J., S. N. Aitken, R. Alía, S. C. González-Martínez, H. Hänninen, A. Kremer, F. Lefèvre, T. Lenormand, S. Yeaman, R. Whetten, and O. Savolainen (2013). Potential for evolutionary responses to climate change - evidence from tree populations. doi:10.1111/gcb.12181.

Albrich, K., W. Rammer, M. G. Turner, Z. Ratajczak, K. H. Braziunas, W. D. Hansen, and R. Seidl (2020). Simulating forest resilience: A review. *Global Ecology and Biogeography*. ISSN 14668238. doi:10.1111/geb.13197.

Arner, S. L., S. Woudenberg, S. Waters, J. Vissage, C. Maclean, M. Thompson, and M. Hansen (2001). National Algorithms for Determining Stocking Class, Stand Size Class, and Forest Type for Forest Inventory and Analysis Plots. Technical report.

Babst, F., O. Bouriaud, B. Poulter, V. Trouet, M. P. Girardin, and D. C. Frank (2019). Twentieth century redistribution in climatic drivers of global tree growth. *Science Advances*, **5**(1). ISSN 2375-2548. doi:10.1126/sciadv.aat4313.

Babst, F., B. Poulter, P. Bodesheim, M. D. Mahecha, and D. C. Frank (2017). Improved tree-ring archives will support earth-system science. *Nature Ecology and Evolution*, **1**(2). ISSN 2397334X. doi:10.1038/s41559-016-0008.

Bates, D., M. Mächler, B. Bolker, and S. Walker (2015). Fitting linear mixed-effects models using lme4. *Journal of Statistical Software*, **67**(1). ISSN 1548-7660. doi:10.18637/jss.v067.i01.

Black, B. A., D. Griffin, P. van der Sleen, A. D. Wanamaker, J. H. Speer, D. C. Frank, D. W. Stahle, N. Pederson, C. A. Copenheaver, V. Trouet, S. Griffin, and B. M. Gillanders (2016). The value of crossdating to retain high-frequency variability, climate signals, and extreme events in environmental proxies. *Global Change Biology*, **22**(7). ISSN 13541013. doi:10.1111/gcb.13256.

Bohner, T. and J. Diez (2019). Extensive mismatches between species distributions and performance and their relationship to functional traits. *Ecology Letters*. ISSN 14610248. doi:10.1111/ele.13396.

Bonan, G. B. (2008). Forests and climate change: Forcings, feedbacks, and the climate benefits of forests. *Science*, **320**(5882). ISSN 0036-8075. doi:10.1126/science.1155121.

Bowman, D. M., R. J. Brienen, E. Gloor, O. L. Phillips, and L. D. Prior (2013). Detecting trends in tree growth: Not so simple. doi:10.1016/j.tplants.2012.08.005.

Brown, J. H. (1984). On the relationship between abundance and distribution of species. *The American Naturalist*, **124**(2). ISSN 0003-0147. doi:10.1086/284267.

Buckman, R. E. (1962). Growth and yield of red pine in Minnesota. Technical report, USDA FS Lake States, St. Paul, MN.

Bunn, A. G. (2008). A dendrochronology program library in R (dplR). *Dendrochronologia*, **26**(2). ISSN 11257865. doi:10.1016/j.dendro.2008.01.002.

Buongiorno, J. and B. R. Michie (1980). A matrix model of uneven-aged forest management. *Forest Science*, **26**(4), pp. 609–625.

Burrill, Ea, Wilson, Am, Turner, Ja, Pugh, Sa, Menlove, Christensen, Conkling, BL, and David (2018). The Forest Inventory and Analysis Database: Database Description and User Guide for Phase 2 (version 8.0). Technical report, USDA Forest Service Forest Inventory and Analysis Program.

Canham, C. D., P. T. LePage, and K. D. Coates (2004). A neighborhood analysis of canopy tree competition: Effects of shading versus crowding. *Canadian Journal of Forest Research*, **34**(4). ISSN 0045-5067. doi:10.1139/x03-232.

Canham, C. D., L. Murphy, R. Riemann, R. McCullough, and E. Burrill (2018). Local differentiation in tree growth responses to climate. *Ecosphere*, **9**(8). ISSN 21508925. doi:10.1002/ecs2.2368.

Cao, Q. and M. Strub (2008). Evaluation of four methods to estimate parameters of an annual tree survival and diameter growth model. *Forest Science*, **54**(6), pp. 617–624.

Cao, Q. V. (2000). Prediction of annual diameter growth and survival for individual trees from periodic measurements. *Forest Science*, **46**(1), pp. 127–131.

Cawrse, D., C. Keyser, T. Keyser, A. Sanchez Meador, E. Smith-Mateja, and M. Van Dyck (2010). Forest Vegetation Simulator Model Validation Protocols. Technical report, USDA Forest Service Forest Management Service Center, Fort Collins, CO.

Cook, E. R. (1985). *A linear aggregate model for tree-ring series*. Ph.D. thesis, The University of Arizona, Tucson, AZ.

Crookston, N. L. and G. E. Dixon (2005). The forest vegetation simulator: A review of its structure, content, and applications. *Computers and Electronics in Agriculture*, **49**(1), pp. 60–80. ISSN 01681699. doi:10.1016/j.compag.2005.02.003.

Crookston, N. L., G. E. Rehfeldt, G. E. Dixon, and A. R. Weiskittel (2010). Addressing climate change in the forest vegetation simulator to assess impacts on landscape forest dynamics. *Forest Ecology and Management*, **260**(7), pp. 1198–1211. ISSN 03781127. doi:10.1016/j.foreco.2010.07.013.

Crookston, N. L., G. E. Rehfeldt, and M. V. Warwell (2005). Using Forest Inventory and Analysis Data To Model Plant-Climate Relationships. In McRoberts, R. E., G. A. Reams, P. C. Van Deusen, and W. H. McWilliams (eds.) *Proceedings of the Seventh Annual Forest Inventory and Analysis Symposium*, volume 23, pp. 243–250. U.S. Department of Agriculture Forest Service, Portland, ME.

Curtis, R. O. (1972). Yield tables past and present. *Journal of Forestry*, **70**(1), pp. 28–32.

Daly, C., M. Halbleib, J. I. Smith, W. P. Gibson, M. K. Doggett, G. H. Taylor, J. Curtis, and P. P. Pasteris (2008). Physiographically sensitive mapping of climatological temperature and precipitation across the conterminous United States. *International Journal of Climatology*, **28**(15). ISSN 08998418. doi:10.1002/joc.1688.

Dannenberg, M. P., E. K. Wise, and W. K. Smith (2019). Reduced tree growth in the semiarid United States due to asymmetric responses to intensifying precipitation extremes. *Science Advances*, **5**(10). ISSN 2375-2548. doi:10.1126/sciadv.aaw0667.

DeRose, R. J., J. D. Shaw, and J. N. Long (2017). Building the forest inventory and analysis tree-ring data set. *Journal of Forestry*, **115**(4), pp. 283–291. ISSN 0022-1201. doi:10.5849/jof.15-097.

Dietze, M. C., A. Fox, L. M. Beck-Johnson, J. L. Betancourt, M. B. Hooten, C. S. Jarnevich, T. H. Keitt, M. A. Kenney, C. M. Laney, L. G. Larsen, H. W. Loescher, C. K. Lunch, B. C. Pijanowski, J. T. Randerson, E. K. Read, A. T. Tredennick, R. Vargas, K. C. Weathers, and E. P. White (2018). Iterative near-term ecological forecasting: Needs, opportunities, and challenges. *Proceedings of the National Academy of Sciences*, **115**(7), pp. 1424–1432. ISSN 0027-8424. doi:10.1073/pnas.1710231115.

Dixon, G. E. (1985). Crown Ratio Modeling Using Stand Density Index and the Weibull Distribution. Technical report, WO Timber Management Staff, Fort Collins, CO.

Dixon, G. E. (2002). Essential FVS: A User's Guide to the Forest Vegetation Simulator. Technical report, USDA FS Forest Management Service Center, Fort Collins, CO.

Dormann, C. F., J. Elith, S. Bacher, C. Buchmann, G. Carl, G. Carré, J. R. G. Marquéz, B. Gruber, B. Lafourcade, P. J. Leitão, T. Münkemüller, C. McClean, P. E. Osborne, B. Reineking, B. Schröder, A. K. Skidmore, D. Zurell, and S. Lautenbach (2013). Collinearity: A review of methods to deal with it and a simulation study evaluating their performance. *Ecography*, **36**(1). ISSN 09067590. doi: 10.1111/j.1600-0587.2012.07348.x.

Ek, A. R. (1974). Nonlinear models for stand table projection in Northern hardwood stands. *Canadian Journal of Forest Research*, **4**(1). ISSN 0045-5067. doi:10.1139/x74-004.

Ek, A. R. and R. A. Monserud (1974). FOREST: A computer model for simulating the growth and reproduction of mixed species forest stands. Technical report, School of Natural Resources, College of Agricultural and Life Sciences, University of Wisconsin, Madison, WI.

Evans, M. R. (2012). Modelling ecological systems in a changing world. *Philosophical Transactions of the Royal Society B: Biological Sciences*, **367**(1586), pp. 181–190. ISSN 14712970. doi:10.1098/rstb.2011.0172.

Fox, J. and S. Weisberg (2019). *An {R} Companion to Applied Regression*. Sage, Thousand Oaks, CA, third edition.

Friedlingstein, P., M. Meinshausen, V. K. Arora, C. D. Jones, A. Anav, S. K. Liddicoat, and R. Knutti (2014). Uncertainties in CMIP5 climate projections due to carbon cycle feedbacks. *Journal of Climate*, **27**(2), pp. 511–526. ISSN 0894-8755. doi:10.1175/JCLI-D-12-00579.1.

Fritts, H. (1976). *Tree rings and climate*. Academic Press, London, UK.

Fritts, H. C., D. G. Smith, J. W. Cardis, and C. A. Budelsky (1965). Tree-ring characteristics along a vegetation gradient in Northern Arizona. *Ecology*, **46**(4). ISSN 00129658. doi:10.2307/1934872.

García, O. (1984). New class of growth models for even-aged stands: Pinus radiata in Golden Downs Forest. *New Zealand Journal of Forest Science*, **14**(1), pp. 65–88.

García, O. (1994). The state-space approach in growth modelling. *Canadian Journal of Forest Research*, **24**(9), pp. 1894–1903.

Gibson, J., G. Moisen, T. Frescino, and T. C. Edwards (2014). Using publicly available forest inventory data in climate-based models of tree species distribution: Examining effects of true versus altered location Coordinates. *Ecosystems*, **17**(1), pp. 43–53. ISSN 14329840. doi:10.1007/s10021-013-9703-y.

Hann, D. W. (1980). Development and evaluation of an even-and uneven-aged ponderosa pine/Arizona fescue stand simulator. Technical report, USDA FS Intermountain Forest and Range Experiment Station, Ogden, UT.

Hofierka, J. and M. Suri (2002). The solar radiation model for open source GIS: Implementation and applications. In *Proceedings of the Open Source GIS-GRASS Users Conference*, pp. 19–. Trento.

Housset, J. M., S. Nadeau, N. Isabel, C. Depardieu, I. Duchesne, P. Lenz, and M. P. Girardin (2018). Tree rings provide a new class of phenotypes for genetic associations that foster insights into adaptation of conifers to climate change. *New Phytologist*, **218**(2), pp. 630–645. ISSN 14698137. doi:10.1111/nph.14968.

Hutchinson, G. E. (1957). Concluding Remarks. *Cold Spring Harbor Symposia on Quantitative Biology*, **22**(0). ISSN 0091-7451. doi:10.1101/SQB.1957.022.01.039.

Hutchinson, G. E. (1978). An introduction to population biology. Technical report, Yale University Press, New Haven, CT.

Keyser, C. E. and G. E. Dixon (2019). Utah (UT) Variant Overview - Forest Vegetation Simulator. Technical report, U.S. Department of Agriculture, Forest Service, Forest Management Service Center, Fort Collins, CO.

Klesse, S., R. J. DeRose, F. Babst, B. A. Black, L. D. Anderegg, J. Axelson, A. Ettinger, H. Griesbauer, C. H. Guiterman, G. Harley, J. E. Harvey, Y. H. Lo, A. M. Lynch, C. O'Connor, C. Restaino, D. Sauchyn, J. D. Shaw, D. J. Smith, L. Wood, J. Villanueva-Díaz, and M. E. Evans (2020). Continental-scale tree-ring-based projection of Douglas-fir growth: Testing the limits of space-for-time substitution. *Global Change Biology*, **26**(9), pp. 5146–5163. ISSN 13652486. doi:10.1111/gcb.15170.

Klesse, S., R. J. DeRose, C. H. Guiterman, A. M. Lynch, C. D. O'Connor, J. D. Shaw, and M. E. K. Evans (2018). Sampling bias overestimates climate change impacts on forest growth in the southwestern United States. *Nature Communications*, **9**(1), p. 5336. ISSN 2041-1723. doi:10.1038/s41467-018-07800-y.

Krajicek, J. E., K. A. Brinkman, and S. F. Gingrich (1961). Crown competition - A measure of density. *Forest Science*, **7**(1), pp. 35–42.

Kuznetsova, A., P. B. Brockhoff, and R. H. B. Christensen (2017). lmerTest package: Tests in linear mixed effects models. *Journal of Statistical Software*, **82**(13). ISSN 1548-7660. doi:10.18637/jss.v082.i13.

Langlet, O. (1971). Two hundred years genecology. *Taxon*, **20**(5-6), pp. 653–721.

Le Quéré, C., R. M. Andrew, P. Friedlingstein, S. Sitch, J. Pongratz, A. C. Manning, J. I. Korsbakken, G. P. Peters, J. G. Canadell, R. B. Jackson, T. A. Boden, P. P. Tans, O. D. Andrews, V. K. Arora, D. C. E. Bakker, L. Barbero, M. Becker, R. A. Betts, L. Bopp, F. Chevallier, L. P. Chini, P. Ciais, C. E. Cosca, J. Cross, K. Currie, T. Gasser, I. Harris, J. Hauck, V. Haverd, R. A. Houghton, C. W. Hunt, G. Hurtt, T. Ilyina, A. K. Jain, E. Kato, M. Kautz, R. F. Keeling, K. Klein Goldewijk, A. Körtzinger, P. Landschützer, N. Lefèvre, A. Lenton, S. Lienert, I. Lima, D. Lombardozzi, N. Metzl, F. Millero, P. M. S. Monteiro, D. R. Munro, J. E. M. S. Nabel, S.-i. Nakaoka, Y. Nojiri, X. A. Padin, A. Peregon, B. Pfeil, D. Pierrot, B. Poulter, G. Rehder, J. Reimer, C. Rödenbeck, J. Schwinger, R. Séférian, I. Skjelvan, B. D. Stocker, H. Tian, B. Tilbrook, F. N. Tubiello, I. T. van der Laan-Luijkx, G. R. van der Werf, S. van Heuven, N. Viovy, N. Vuichard, A. P. Walker, A. J. Watson, A. J. Wiltshire, S. Zaehle, and D. Zhu (2018). Global carbon budget 2017. *Earth System Science Data*, **10**(1). ISSN 1866-3516. doi:10.5194/essd-10-405-2018.

Le Quéré, C., R. Moriarty, R. M. Andrew, J. G. Canadell, S. Sitch, J. I. Korsbakken, P. Friedlingstein, G. P. Peters, R. J. Andres, T. A. Boden, R. A. Houghton, J. I. House, R. F. Keeling, P. Tans, A. Arneth, D. C. E. Bakker, L. Barbero, L. Bopp, J. Chang, F. Chevallier, L. P. Chini, P. Ciais, M. Fader, R. A. Feely, T. Gkritzalis, I. Harris, J. Hauck, T. Ilyina, A. K. Jain, E. Kato, V. Kitidis, K. Klein Goldewijk, C. Koven, P. Landschützer, S. K. Lauvset, N. Lefèvre, A. Lenton, I. D. Lima, N. Metzl, F. Millero, D. R. Munro, A. Murata, J. E. M. S. Nabel, S. Nakaoka, Y. Nojiri, K. O'Brien, A. Olsen, T. Ono, F. F. Pérez, B. Pfeil, D. Pierrot, B. Poulter, G. Rehder, C. Rödenbeck, S. Saito, U. Schuster, J. Schwinger, R. Séférian, T. Steinhoff, B. D. Stocker, A. J. Sutton, T. Takahashi, B. Tilbrook, I. T. van der Laan-Luijkx, G. R. van der Werf, S. van Heuven, D. Vandemark, N. Viovy, A. Wiltshire, S. Zaehle, and N. Zeng (2015). Global carbon budget 2015. *Earth System Science Data*, **7**(2), pp. 349–396. ISSN 1866-3516. doi:10.5194/essd-7-349-2015.

Leites, L. P., A. P. Robinson, G. E. Rehfeldt, J. D. Marshall, and N. L. Crookston (2012). Height-growth response to climatic changes differs among populations of Douglas-fir: a novel analysis of historic data. *Ecological Applications*, **22**(1), pp. 154–165.

Leslie, P. H. (1945). On the use of matrices in certain population mathematics. *Biometrika*, **33**, pp. 183–212.

MacKinney, A. L., F. X. Schumacher, and L. E. Chaiken (1937). Construction of yield tables for non-normal loblolly pinestands. *Journal of Agricultural Research*, **54**, pp. 531–545.

Maguire Jr, B. (1973). Niche response structure and the analytical potentials of its relationship to the habitat. *The American Naturalist*, **107**(954), pp. 213–246.

Martin-Benito, D., V. Kint, M. del Río, B. Muys, and I. Cañellas (2011). Growth responses of West-Mediterranean Pinus nigra to climate change are modulated by competition and productivity: Past trends and future perspectives. *Forest Ecology and Management*, **262**(6), pp. 1030–1040. ISSN 03781127. doi:10.1016/j.foreco.2011.05.038.

McCullough, I. M., F. W. Davis, and A. P. Williams (2017). A range of possibilities: Assessing geographic variation in climate sensitivity of ponderosa pine using tree rings. *Forest Ecology and Management*, **402**, pp. 223–233. ISSN 03781127. doi:10.1016/j.foreco.2017.07.025.

McGill, B. J. (2012). Trees are rarely most abundant where they grow best. *Journal of Plant Ecology*, **5**(1). ISSN 1752-9921. doi:10.1093/jpe/rtr036.

Milner, K. S., D. W. Coble, A. J. McMahan, and E. L. Smith (2003). FVSBGC: A hybrid of the physiological model STAND-BGC and the forest vegetation simulator. In *Canadian Journal of Forest Research*, volume 33, pp. 466–479. ISSN 00455067. doi:10.1139/x02-161.

Mina, M., D. Martin-Benito, H. Bugmann, and M. Cailleret (2016). Forward modeling of tree-ring width improves simulation of forest growth responses to drought. *Agricultural and Forest Meteorology*, **221**. ISSN 01681923. doi:10.1016/j.agrformet.2016.02.005.

Monserud, R. A. (1984). Height growth and site index curves for inland Douglas-fir based on stem analysis data and forest habitat type. *Forest Science*, **30**(4), pp. 943–965.

Monserud, R. A. and H. Sterba (1996). A basal area increment model for individual trees growing in even- and uneven-aged forest stands in Austria. *Forest Ecology and Management*, **80**(1-3). ISSN 03781127. doi:10.1016/0378-1127(95)03638-5.

Monserud, R. A., Y. Yang, S. Huang, and N. Tchebakova (2008). Potential change in lodgepole pine site index and distribution under climatic change in Alberta. *Canadian Journal of Forest Research*, **38**(2), pp. 343–352. ISSN 00455067. doi:10.1139/X07-166.

Moore, P. T., R. J. DeRose, J. N. Long, and H. van Miegroet (2012). Using silviculture to influence carbon sequestration in Southern Appalachian spruce-fir forests. *Forests*, **3**(2), pp. 300–316. ISSN 19994907. doi:10.3390/f3020300.

National Academies of Sciences, E. and Medicine (2019). *Negative Emissions Technologies and Reliable Sequestration*. National Academies Press, Washington, D.C. ISBN 978-0-309-48452-7. doi:10.17226/25259.

Pagel, J., M. Treurnicht, W. J. Bond, T. Kraaij, H. Nottebrock, A. Schutte-Vlok, J. Tonnabel, K. J. Esler, and F. M. Schurr (2020). Mismatches between demographic niches and geographic distributions are strongest in poorly dispersed and highly persistent plant species. *Proceedings of the National Academy of Sciences*, **117**(7). ISSN 0027-8424. doi:10.1073/pnas.1908684117.

Pan, Y., R. A. Birdsey, J. Fang, R. Houghton, P. E. Kauppi, W. A. Kurz, O. L. Phillips, A. Shvidenko, S. L. Lewis, J. G. Canadell, P. Ciais, R. B. Jackson, S. W. Pacala, A. D. McGuire, S. Piao, A. Rautiainen, S. Sitch, and D. Hayes (2011). A large and persistent carbon sink in the world's forests. *Science*, **333**(6045). ISSN 0036-8075. doi:10.1126/science.1201609.

Park Williams, A., C. D. Allen, A. K. Macalady, D. Griffin, C. A. Woodhouse, D. M. Meko, T. W. Swetnam, S. A. Rauscher, R. Seager, H. D. Grissino-Mayer, J. S. Dean, E. R. Cook, C. Gangodagamage, M. Cai, and N. G. McDowell (2013). Temperature as a potent driver of regional forest drought stress and tree mortality. *Nature Climate Change*, **3**(3). ISSN 1758-678X. doi:10.1038/nclimate1693.

Peng, C. (2000). Growth and yield models for uneven-aged stands: Past, present and future. *Forest Ecology and Management*, **132**, pp. 259–279.

Pickett, S. T. A. (1989). Space-for-time substitution as an alternative to long-term studies. In Likens, G. E. (ed.) *Long-term studies in ecology: Approaches and alternatives*, chapter 5, pp. 110–135. Springer, New York, NY.

Piñeiro, G., S. Perelman, J. P. Guerschman, and J. M. Paruelo (2008). How to evaluate models: Observed vs. predicted or predicted vs. observed? *Ecological Modelling*, **216**(3-4). ISSN 03043800. doi:10.1016/j.ecolmodel.2008.05.006.

Pironon, S., G. Papuga, J. Villellas, A. L. Angert, M. B. García, and J. D. Thompson (2016). Geographic variation in genetic and demographic performance: New insights from an old biogeographical paradigm. *Biological Reviews*, **92**(4), pp. 1877–1909. ISSN 1469185X. doi:10.1111/brv.12313.

Pironon, S., J. Villellas, W. Thuiller, V. M. Eckhart, M. A. Geber, D. A. Moeller, and M. B. García (2018). The 'Hutchinsonian niche' as an assemblage of demographic

niches: Implications for species geographic ranges. *Ecography*, **41**(7), pp. 1103–1113. ISSN 16000587. doi:10.1111/ecog.03414.

Pokharel, B. and R. E. Froese (2008). Evaluating alternative implementations of the Lake States FVS diameter increment model. *Forest Ecology and Management*, **255**(5-6), pp. 1759–1771. ISSN 03781127. doi:10.1016/j.foreco.2007.11.035.

Porté, A. and H. H. Bartelink (2002). Modelling mixed forest growth: A review of models for forest management. *Ecological Modelling*, **150**, pp. 141–188.

Pretzsch, H. and P. Biber (2010). Size-symmetric versus size-asymmetric competition and growth partitioning among trees in forest stands along an ecological gradient in central Europe. *Canadian Journal of Forest Research*, **40**(2). ISSN 0045-5067. doi:10.1139/X09-195.

Prisley, S. P., H.-J. Wang, P. J. Radtke, and J. Coulston (2009). Combining FIA Plot Data with Topographic Variables: Are Precise Locations Needed? U.S. Department of Agriculture, Forest Service, Rocky Mountain Research Station, U.S. Department of Agriculture, Forest Service, Rocky Mountain Research Station, Fort Collins, CO.

Puhlick, J. J., A. R. Weiskittel, L. S. Kenefic, C. W. Woodall, and I. J. Fernandez (2020). Strategies for enhancing long-term carbon sequestration in mixed-species, naturally regenerated Northern temperate forests. *Carbon Management*, pp. 1–17. ISSN 17583012. doi:10.1080/17583004.2020.1795599.

Reclamation (2014). Downscaled CMIP3 and CMIP5 Climate and Hydrology Projections: Release of Hydrology Projections, Comparison with preceding Information, and Summary of User Needs. Technical report, U.S. Department of the Interior, Bureau of Reclamation, Technical Services Center, Denver, Colorado.

Rehfeldt, G. E., N. L. Crookston, M. V. Warwell, and J. S. Evans (2006). Empirical analyses of plant-climate relationships for the Western United States. *International Journal of Plant Sciences*, **167**(6), pp. 1123–1150.

Reineke, L. (1933). Perfecting a stand-density index for even-aged forests . *Journal of Agricultural Research*, **46**, pp. 627–638.

Schielzeth, H. (2010). Simple means to improve the interpretability of regression coefficients. *Methods in Ecology and Evolution*, **1**(2), pp. 103–113. doi:10.1111/j.2041-210x.2010.00012.x.

Seyednasrollah, B. (2018). solrad: To calculate solar radiation and related variables based on location, time and topographical conditions.

Shaw, J. D. (2000). Application of stand density index to irregularly structured stands. *Western Journal of Applied Forestry*, **15**(1), pp. 40–42.

Shifley, S. R., H. S. He, H. Lischke, W. J. Wang, W. Jin, E. J. Gustafson, J. R. Thompson, F. R. Thompson, W. D. Dijak, and J. Yang (2017). The past and future of modeling forest dynamics: From growth and yield curves to forest landscape models. *Landscape Ecology*, **32**(7), pp. 1307–1325. ISSN 15729761. doi: 10.1007/s10980-017-0540-9.

Snell, R. S., A. Huth, J. E. Nabel, G. Bocedi, J. M. Travis, D. Gravel, H. Bugmann, A. G. Gutiérrez, T. Hickler, S. I. Higgins, B. Reineking, M. Scherstjanoi, N. Zurbriggen, and H. Lischke (2014). Using dynamic vegetation models to simulate plant range shifts. *Ecography*, **37**(12), pp. 1184–1197. ISSN 16000587. doi:10.1111/ecog.00580.

Somerville, W. (1891). An account of Pressler's growth-borer. *Botanical Society of Edinburgh*, **19**, pp. 90–93.

Speer, J. H. (2010). *Fundamentals of tree-ring research*. University of Arizona Press, Tucson, AZ.

Stage, A. R. (1968). A tree-by-tree measure of site utilization for grand fir related to stand density index. Technical report, USDA Forest Service Research Note INT-77.

Stage, A. R. (1973). Prognosis model for stand development. Technical report, USDA FS Intermountain Forest and Range Experiment Station., Ogden, UT.

Swetnam, T. W., C. D. Allen, and J. L. Betancourt (1999). Applied historical ecology: Using the past to manage for the future. *Ecological Applications*, **9**(4), pp. 1189–1206.

Thuiller, W., T. Münkemüller, K. H. Schiffers, D. Georges, S. Dullinger, V. M. Eckhart, T. C. Edwards, D. Gravel, G. Kunstler, C. Merow, K. Moore, C. Piedallu, S. Vissault, N. E. Zimmermann, D. Zurell, and F. M. Schurr (2014). Does probability of occurrence relate to population dynamics? *Ecography*, **37**(12). ISSN 09067590. doi:10.1111/ecog.00836.

Tinkham, W. T., P. R. Mahoney, A. T. Hudak, G. M. Domke, M. J. Falkowski, C. W. Woodall, and A. M. Smith (2018). Applications of the United States Forest Inventory and Analysis dataset: A review and future directions. *Canadian Journal of Forest Research*, **48**, pp. 1251–1268. doi:https://doi.org/10.1139/cjfr-2018-0196.

Tolwinski-Ward, S. E., M. N. Evans, M. K. Hughes, and K. J. Anchukaitis (2011). An efficient forward model of the climate controls on interannual variation in

tree-ring width. *Climate Dynamics*, **36**(11-12). ISSN 0930-7575. doi:10.1007/s00382-010-0945-5.

US Department of Agriculture, F. S. (2020). Forest Inventory and Analysis National Core Field Guide Volume I: Field Data Collection Procedures for Phase 2 Plots. Technical report.

Usher, M. B. (1966). A matrix approach to the management of renewable resources, with special reference to selection forests. *The Journal of Applied Ecology*, **3**(2). ISSN 00218901. doi:10.2307/2401258.

Usher, M. B. (1969). A matrix model for forest management. *Biometrics*, **25**(2). ISSN 0006341X. doi:10.2307/2528791.

Vuokila, Y. (1965). Functions for variable density yield tables of pine based on temporary sample plots.

Walters, C. (1986). *Adaptive Management of Renewable Resources*. Macmillan Publishing Company, New York.

Weiskittel, A. R., S. M. Garber, G. P. Johnson, D. A. Maguire, and R. A. Monserud (2007). Annualized diameter and height growth equations for Pacific Northwest plantation-grown Douglas-fir, western hemlock, and red alder. *Forest Ecology and Management*, **250**, pp. 266–278.

Weiskittel, A. R., D. W. Hann, J. Kershaw, John A., and J. K. Vanclay (2011). *Forest Growth and Yield Modeling*. John Wiley & Sons, Incorporated, New York, 1 edition.

Wykoff, W. R., N. L. Crookston, and A. R. Stage (1982). User's Guide to the Stand Prognosis Model. Technical report, USDA FS Intermountain Forest and Range Experiment Station, Ogden, UT.

Zang, C. and F. Biondi (2015). treeclim: An R package for the numerical calibration of proxy-climate relationships. *Ecography*, **38**(4). ISSN 09067590. doi:10.1111/ecog.01335.